*J Neurophysiol* 107: 159–177, 2012.
First published September 28, 2011; doi:10.1152/jn.00653.2011.

# Task-level feedback can explain temporal recruitment of spatially fixed muscle synergies throughout postural perturbations

**Seyed A. Safavynia[1,2] and Lena H. Ting[1,3]**

[1]*Neuroscience Program, Emory University,* [2]*Medical Scientist Training Program, Emory University School of Medicine, and* [3]*The Wallace H. Coulter Department of Biomedical Engineering, Georgia Institute of Technology and Emory University, Atlanta, Georgia*

Submitted 13 July 2011; accepted in final form 22 September 2011

**Safavynia SA, Ting LH.** Task-level feedback can explain temporal recruitment of spatially fixed muscle synergies throughout postural perturbations. *J Neurophysiol* 107: 159–177, 2012. First published September 28, 2011; doi:10.1152/jn.00653.2011.—Recent evidence suggests that complex spatiotemporal patterns of muscle activity can be explained with a low-dimensional set of muscle synergies or M-modes. While it is clear that both spatial and temporal aspects of muscle coordination may be low dimensional, constraints on spatial versus temporal features of muscle coordination likely involve different neural control mechanisms. We hypothesized that the low-dimensional spatial and temporal features of muscle coordination are independent of each other. We further hypothesized that in reactive feedback tasks, spatially fixed muscle coordination patterns—or muscle synergies—are hierarchically recruited via time-varying neural commands based on delayed task-level feedback. We explicitly compared the ability of spatially fixed (SF) versus temporally fixed (TF) muscle synergies to reconstruct the entire time course of muscle activity during postural responses to anterior-posterior support-surface translations. While both SF and TF muscle synergies could account for EMG variability in a postural task, SF muscle synergies produced more consistent and physiologically interpretable results than TF muscle synergies during postural responses to perturbations. Moreover, a majority of SF muscle synergies were consistent in structure when extracted from epochs throughout postural responses. Temporal patterns of SF muscle synergy recruitment were well-reconstructed by delayed feedback of center of mass (CoM) kinematics and reproduced EMG activity of multiple muscles. Consistent with the idea that independent and hierarchical low-dimensional neural control structures define spatial and temporal patterns of muscle activity, our results suggest that CoM kinematics are a task variable used to recruit SF muscle synergies for feedback control of balance.

balance; center of mass; electromyography; motor control

A FUNDAMENTAL PROBLEM in motor control is how the central nervous system (CNS) chooses among an overabundant set of muscles and joints to execute a movement (Bernstein 1967). Recent evidence in a variety of tasks across species suggests that complex spatiotemporal patterns of muscle activity can be explained with a low-dimensional set of muscle synergies (Cheung et al. 2005; d'Avella and Bizzi 2005; Hart and Giszter 2004; Ivanenko et al. 2005; Krouchev et al. 2006; Saltiel et al. 2001; Ting and Macpherson 2005; Torres-Oviedo and Ting 2007; Tresch et al. 1999). However, previous analyses have either identified low-dimensional structures that constrain the spatial groupings of muscles, leaving temporal patterns unconstrained (Fig. 1*A*) (Hart and Giszter 2004; Saltiel et al. 2001; Torres-Oviedo and Ting 2007) or identified low-dimensional structure in the temporal features of muscle activity, leaving spatial patterns unconstrained (Fig. 1*B*) (Cappellini et al. 2006; Ivanenko et al. 2004, 2005). Although both spatial and temporal constraints on muscle coordination may be low dimensional, they likely involve different neural control mechanisms (Ivanenko et al. 2005; Kargo and Giszter 2000; Kargo et al. 2010; McCrea and Rybak 2008). Specifically, in postural responses to perturbations, temporal muscle activation patterns are due to task-level sensorimotor feedback (Welch and Ting 2008), as opposed to feedforward temporal patterns that may drive locomotor behaviors.

A number of studies have proposed that muscle synergies have spatially fixed muscle weightings but are subject to time-varying temporal recruitment (Clark et al. 2010; Hart and Giszter 2004; Kargo et al. 2010). In this organization, a spatially fixed (SF) muscle synergy represents a group of muscles with fixed ratios of activation that can be recruited by variable temporal neural commands to execute a task in a feedforward or feedback manner (Fig. 1*A*). SF muscle synergies are recruited across a range of locomotor tasks with varying temporal recruitment patterns (Clark et al. 2010; d'Avella and Bizzi 2005). For example, changes in the temporal recruitment of SF muscle synergies can vary from step to step in human walking, as well as systematically across a range of speeds (Clark et al. 2010). In reactive tasks, altered temporal recruitment patterns of SF muscle synergies account for many directions of movement and postural configurations (Hart and Giszter 2004; Kargo and Giszter 2000; Ting and Macpherson 2005; Torres-Oviedo et al. 2006; Torres-Oviedo and Ting 2007, 2010). However, in our previous studies of balance control, analyses of SF muscle synergy recruitment were limited to gross variations in a few large time bins (~75 ms) during the initial portion of the postural response. It remains unclear whether SF muscle synergies can account for the finer dynamics of muscle activity throughout the entire postural response, including later periods that are more heavily influenced by ongoing body motion and descending commands.

It has been alternatively proposed that muscle synergies are temporally fixed patterns of muscle recruitment that are coupled to spatially varying muscle weightings (Cappellini et al. 2006; Ivanenko et al. 2004, 2005). In a temporally fixed (TF) muscle synergy organization, rhythmic motor patterns are constructed in a feedforward manner through a set of predefined temporal recruitment patterns that activate variable spatial patterns of muscle activity across conditions (Fig. 1*B*).

Address for reprint requests and other correspondence: L. H. Ting, Wallace H. Coulter Dept. of Biomedical Engineering, Georgia Inst. of Technology and Emory Univ., 313 Ferst Dr., Atlanta, GA 30332-0535 (e-mail: lting@emory.edu).

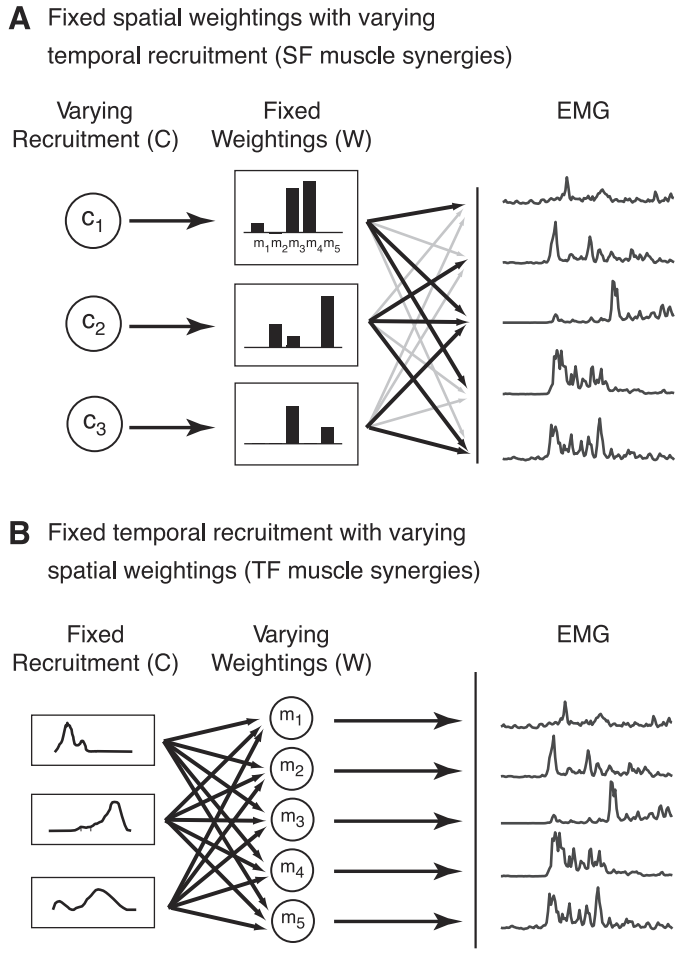


Fig. 1. Hypotheses and concepts explored in the present study. *A*: muscle synergies with fixed spatial weightings [spatially fixed (SF) muscle synergies]. Here the nervous system organizes muscle activity spatially. The nervous system can variably recruit SF muscle synergies when a specific muscle combination is desired throughout a task in a feedback or feedforward manner. *B*: muscle synergies with fixed temporal recruitment [temporally fixed (TF) muscle synergies]. In this hypothesis, the nervous system uses fixed temporal sequences to recruit muscles during a task, consistent with feedforward control. When a specific temporal sequence is executed, a set of muscles that can vary across directions and trials is chosen to reproduce EMG activity necessary to achieve the task.

In locomotion, a few temporal patterns can be recruited across step cycles to reproduce electromyographic (EMG) patterns across different walking speeds (Ivanenko et al. 2004) and when walking is combined with other voluntary tasks (Ivanenko et al. 2005). However, it may not be possible to dissociate spatial from temporal organization during cyclical locomotor tasks where temporal and spatial features of muscle activity tend to be correlated.

Recent evidence suggests that low-dimensional temporal patterns may be used to recruit SF muscle synergies. For example, fixed-duration temporal pulses are sufficient to explain muscle activation patterns described by SF muscle synergies in frog preparations (Hart and Giszter 2004). Similarly, temporal patterns of muscle activity in postural perturbations during balance are defined by a low-dimensional sensorimotor transformation based on feedback control of center of mass (CoM) motion (Lockhart and Ting 2007; Welch and Ting 2008, 2009). CoM kinematics are task-level variables that must be estimated from multisensory integration (Peterka 2002) and encapsulate the net motion of the body. By assigning unique feedback gains to CoM displacement, velocity, and acceleration for each muscle at a common delay, the model can reconstruct the entire time course of muscle activity in multiple muscles throughout the leg and trunk (Lockhart and Ting 2007; Welch and Ting 2008, 2009). Moreover, the model can explain temporal patterns of muscle activity that vary with perturbation characteristics. While it is unknown whether this model can be used to describe the recruitment of SF muscle synergies, CoM feedback likely recruits SF muscle synergies because SF muscle synergies produce forces necessary for CoM control across a range of postural configurations (Chvatal et al. 2011; McKay and Ting 2008; Ting and Macpherson 2005; Torres-Oviedo et al. 2006). A hierarchical structure in which low-dimensional temporal patterns recruit spatial structures defining muscle activation patterns is also consistent with current theories about locomotor pattern generation (Hart and Giszter 2004; McCrea and Rybak 2008) and trajectory formation (Berniker et al. 2009; Kargo et al. 2010).

Here we hypothesized that during human balance control, low-dimensional temporal feedback mechanisms recruit SF muscle synergies. Specifically, we predicted that SF muscle synergies are modulated by delayed feedback of CoM throughout perturbation responses. To test this hypothesis, we examined muscle synergy structure and recruitment in 10-ms bins throughout postural responses to support-surface translations including later, previously unexplored epochs that extend beyond perturbation deceleration and feature very different combinations of muscle activity and CoM kinematics compared with the initial postural response. We explicitly compared SF versus TF muscle synergies on their ability to reconstruct EMG activity in reactive postural responses. We then analyzed the structure and recruitment of SF muscle synergies extracted from epochs throughout postural responses to perturbations. We predicted that SF muscle synergies would have consistent structure regardless of the extraction epoch. Furthermore, we predicted that a feedback model based on CoM kinematics would be able to reproduce SF muscle synergy recruitment patterns and reliably reconstruct SF muscle synergy activity throughout postural responses to perturbations.

## METHODS

### *Summary*

To determine the organization and control of muscle synergies throughout a postural task, we recorded human postural responses to multidirectional ramp-and-hold translations of the support surface. We investigated different hypotheses on muscle synergy organization by extracting both SF and TF muscle synergies from the entire postural response. We compared SF versus TF muscle synergy structure and EMG reconstructions. We then compared SF muscle synergy structures across epochs to determine their degree of consistency across the time course of postural responses. We investigated task-level control of SF muscle synergies by applying a delayed feedback model based on CoM kinematics to reconstruct muscle synergy recruitment throughout anterior-posterior (A-P) perturbations. We compared observed and reconstructed SF muscle synergy recruitment patterns and examined the ability of the feedback model to reconstruct trial-by-trial variability in SF muscle synergy recruitment. To ensure that our models of SF muscle synergy recruitment were adequate to

describe actual EMG data, we reconstructed individual muscle activity from reconstructed SF muscle synergy recruitment patterns.

*Data Collection*

Eight healthy subjects (5 men, 3 women; mean age ± SD: 23.5 ± 2 yr) were exposed to ramp-and-hold perturbations according to an experimental protocol approved by the Georgia Tech and Emory University Institutional Review Boards. Subjects stood on a platform that translated in 12 directions in the horizontal plane. To minimize anticipatory adjustments while maximizing EMG variability, 5 repetitions were randomly presented over 12 directions for a total of 60 trials. Translations were 12.4 cm in displacement, 35 cm/s in velocity, and 0.5 g in acceleration.

EMG activity was recorded from 16 muscles on the right leg and trunk. The muscles included rectus abdominis (REAB), tensor fascia lata (TFL), tibialis anterior (TA), semitendinosus (SEMT), biceps femoris, long head (BFLH), rectus femoris (RFEM), peroneus (PERO), medial gastrocnemius (MGAS), lateral gastrocnemius (LGAS), erector spinae (ERSP), external oblique (EXOB), gluteus medius (GMED), vastus lateralis (VLAT), vastus medialis (VMED), soleus (SOL), and adductor magnus (ADMG). Raw EMG data were collected at 1,080 Hz and then processed according to custom MATLAB routines. Data were high-pass filtered at 35 Hz, de-meaned, rectified, and then low-pass filtered at 40 Hz. Kinematic and kinetic data were also collected for an estimation of CoM. Kinetic data were collected at 1,080 Hz from force plates under the feet (AMTI, Watertown, MA), and kinematic data were collected at 120 Hz with a six-camera Vicon motion capture system (Centennial, CO) and a custom 25-marker set that included head-arms-trunk (HAT), thigh, shank, and foot segments. CoM displacement and velocity were calculated from kinematic data as a weighted sum of segmental masses (Winter 2005); CoM acceleration was calculated from ground reaction forces ($\mathbf{F} = m\mathbf{a}$).

*Data Processing*

To test whether postural responses could be explained with a SF versus a TF muscle synergy organization, it was necessary to account for muscle activity with high resolution. Therefore, for each trial, EMG data were parsed into 10-ms bins in which mean EMG activity was found. Each muscle was normalized to maximum EMG activity across all epochs and perturbation directions for visualization purposes. A data matrix was assembled for EMG activity during the entire perturbation response (100–800 ms after perturbation onset) over all trials, resulting in (70 time bins × 12 directions × 5 repetitions) = 4,200 points for each of 16 muscles. Note that because postural muscle activity begins ~100 ms after a perturbation (Horak and Macpherson 1996), EMG epochs were chosen at a delay of 100 ms with respect to platform motion.

To further test the hypothesis that muscle synergies are spatially invariant, EMG data from the entire perturbation were further analyzed in four smaller epochs corresponding to platform acceleration (*start*; 100–250 ms after platform onset), maximum platform velocity (*plateau*; 250–450 ms after onset), platform deceleration (*stop*; 450–600 ms), and after deceleration (*stable*; 600–800 ms) (Fig. 2). We did not include a background epoch because background EMG was <5% of maximum activity; thus SF muscle synergies were more likely accounting for noise than relevant features of this quiescent data set. SF muscle synergies from the entire perturbation were able to reconstruct background EMG within 10% of actual EMG.

*Muscle Synergy Extraction*

We used nonnegative matrix factorization (NNMF) to extract both SF and TF muscle synergies from EMG activity throughout postural responses to perturbations (Lee and Seung 1999; Ting and Chvatal 2010). The NNMF algorithm is a linear decomposition technique that decomposes an original EMG matrix $\mathbf{E}$ into spatial muscle weightings $\mathbf{W}$ and temporal recruitment patterns $\mathbf{C}$. The NNMF algorithm chooses nonnegative matrices $\mathbf{W}$ and $\mathbf{C}$ at random initially and modifies their composition to minimize the sum of squared errors between the actual ($\mathbf{E}$) and reconstructed ($\mathbf{E}^*$) EMG matrices as shown below:

$$\mathbf{E} = \mathbf{WC} + \text{error}$$

$$\text{error} = \sum_i \sum_j \left(\mathbf{E}_{ij} - \mathbf{E}^*_{ij}\right)^2$$

For a prespecified number of muscle synergies $N_{syn}$, the activity of a muscle $\mathbf{M}_i$ is reconstructed by linearly combining muscle weightings $\mathbf{W}_i$ with temporal recruitment patterns $\mathbf{C}$ according to the equation

$$\mathbf{M}_i = \sum_{j=1}^{N_{syn}} w_{i,j}\mathbf{C}_j$$

For SF muscle synergies, the muscular composition of muscle synergies, $\mathbf{W}$, does not change, although their recruitment coefficients, $\mathbf{C}$, can vary at each time point for each trial. By contrast, for TF muscle synergies, the temporal recruitment patterns $\mathbf{C}$ do not change, although their muscular compositions $\mathbf{W}$ can change across conditions (Fig. 1).

*SF muscle synergies.* To test the hypothesis that muscle synergies have fixed spatial weightings with varying temporal recruitment, we used NNMF to extract SF muscle synergies from EMG data matrices as previously used in postural responses (Torres-Oviedo et al. 2006). In this case, the muscular composition of SF muscle synergies $\mathbf{W}$ is held fixed, and the temporal recruitment coefficients $\mathbf{C}$ can vary at each time point for each trial. We constructed our EMG data matrix to have the dimensions $m \times s$, where $m$ is the number of muscles and $s$ is the number of samples (bins × directions × repetitions). This ensured that the NNMF algorithm would yield spatially fixed muscle weightings $\mathbf{W}$ ($m \times n$ matrix) with varying temporal recruitment coefficients $\mathbf{C}$ ($n \times s$ matrix). We then scaled the rows of the data matrix to have unit variance, weighting the variance of each muscle equally.

We extracted SF muscle synergies $\mathbf{W}$ from 60% of trials and reconstructed muscle activity in all trials. Keeping the muscle weightings $\mathbf{W}$ constant, we varied temporal recruitment coefficients $\mathbf{C}$ to minimize the sum of squared errors between actual and reconstructed EMG patterns. Although we further extracted SF muscle synergies from individual epochs of trials, we ensured that the same set of trials was used for extraction and validation. To compare SF muscle synergy structure across different epochs, we took the unit variance scaling factors from the *start* epoch data matrix and applied them to all data matrices for a subject. We then ran the NNMF algorithm; after the algorithm was complete, we unscaled the data and normalized each SF muscle synergy to its maximum muscle composition, resulting in muscle compositions between 0 and 1.

*TF muscle synergies.* To compare the results of SF muscle synergies against the hypothesis that muscle synergies have fixed temporal recruitment patterns with varying spatial muscle activation, we also extracted TF muscle synergies to yield fixed temporal recruitment patterns. In this case, the matrix $\mathbf{C}$ specifies the fixed temporal recruitment patterns, and the weighting coefficients $\mathbf{W}$ can change across conditions. We constructed our EMG data matrix to have dimension $t \times r$, where $t$ is the number of time points and $r$ is the number of (muscles × directions × trials), so that the NNMF algorithm would yield temporally fixed recruitment patterns $\mathbf{C}$ ($t \times n$ matrix) with spatially varying weightings $\mathbf{W}$ ($n \times r$ matrix) (Ivanenko et al. 2003). To weight the variance of each muscle equally, we reshaped the data matrix to have individual muscle activity in columns, scaled the columns of the matrix to have unit variance, and then restored the original dimensions.

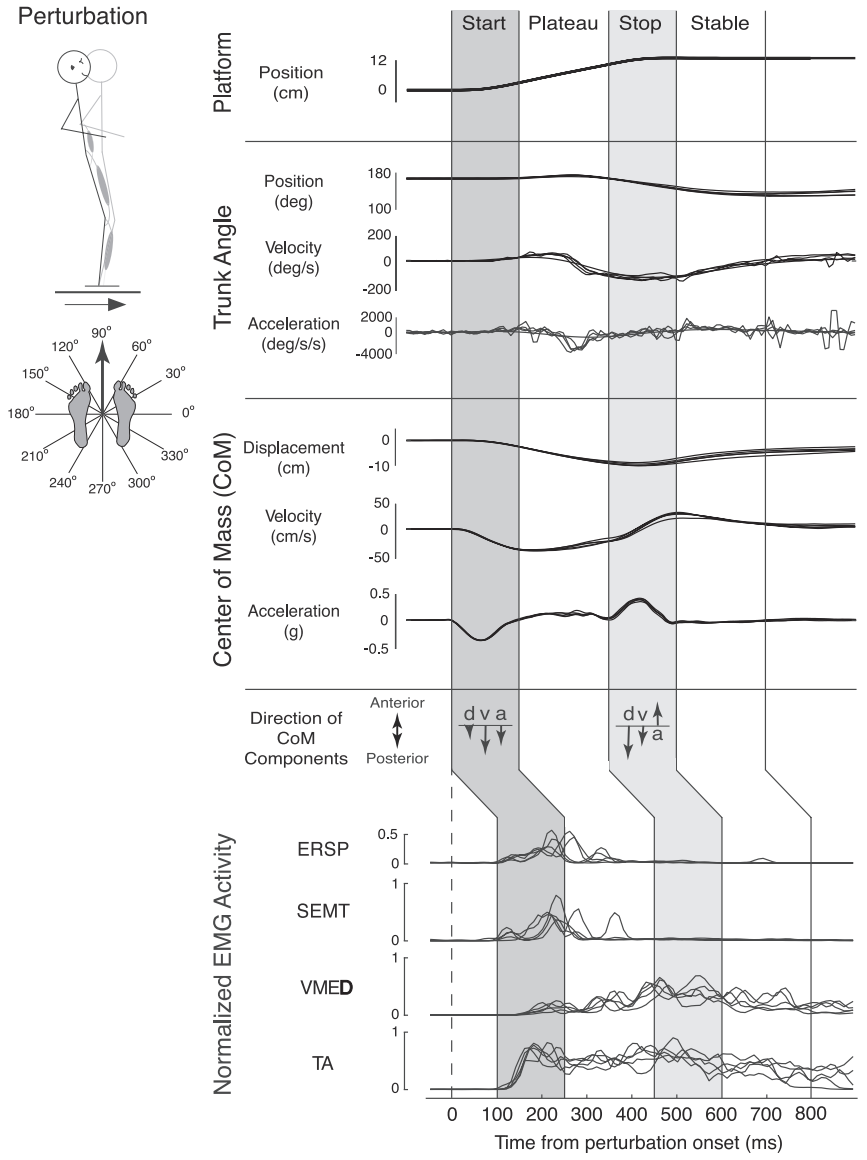


Fig. 2. Representative postural response to a forward ramp-and-hold perturbation. Subjects exhibit motion of individual joints as well as center of mass (CoM) and activate muscles over body segments in response to a forward (90°) perturbation. Initially (*start* epoch), CoM kinematics [displacement (d), velocity (v), acceleration (a)] were all opposite the direction of platform motion. However, when the platform decelerated (*stop* epoch), CoM acceleration was in the opposite direction of CoM displacement and velocity. Intermuscular coordination patterns also changed throughout the perturbations; the major muscles activated in the *start* epoch [tibialis anterior (TA), erector spinae (ERSP), semitendinosus (SEMT)] were different from those activated in the *stop* epoch [TA, vastus medialis (VMED)]. Overlaid muscle traces shown are for individual trials (5 total).

We extracted TF muscle synergies from EMG activity in all directions and trials throughout postural responses to perturbations. For validation purposes, we extracted TF muscle synergies from 60% of trials and reconstructed muscle activity in all trials. Keeping the temporal recruitment patterns **C** constant, we varied muscle weighting coefficients **W** to minimize the sum of squared errors between actual and reconstructed EMG patterns. We ran the NNMF algorithm and subsequently unscaled the data matrix to remove unit variance. Finally, we normalized the TF muscle synergies to their maximum level of activation, yielding a value between 0 and 1 for each TF muscle synergy.

### *Determination of Number of Muscle Synergies*

We extracted 1–10 SF and TF muscle synergies throughout postural responses to perturbations in each subject, and further extracted 1–10 SF muscle synergies from individual epochs of the postural response in each subject. For each data set, goodness of fit between actual and reconstructed EMG was quantified with variability accounted for (VAF), defined as 100 × uncentered Pearson's coefficient of determination (Zar 1999). VAF was evaluated both globally and for all active muscles, ensuring the reproduction of relevant features of the data set. While total VAF evaluates the entire data matrix as a whole, muscle VAF evaluates individual muscles over directions, time bins, and repetitions.

We used a combination of global and local criteria (Chvatal et al. 2011; Torres-Oviedo et al. 2006; Torres-Oviedo and Ting 2007, 2010) to determine the fewest number of SF ($N_{syn\text{-}S}$) or TF ($N_{syn\text{-}T}$) muscle synergies needed to faithfully reconstruct the EMG data matrix. For each data set, we quantified the ability of SF versus TF muscle synergies to account for the variability in the entire data set (total VAF). We also quantified the ability of SF versus TF muscle synergies to account for the variability in individual muscles (muscle VAF). The number of SF or TF muscle synergies was increased as long as total VAF and VAF across muscles improved. However, additional SF or TF muscle synergies that contributed evenly to the VAF across muscles were not included because they likely represented noise in the data as opposed to variations between trials or muscles. VAF of $N_{syn\text{-}S}$ and $N_{syn\text{-}T}$ was ≥75% for each subject overall and for the majority of active muscles (~14 of 16) in all perturbation epochs. A previously established criterion for choosing the number of TF muscle synergies was to include TF muscle synergies until the total VAF improved by <3% (Ivanenko et al. 2005). When applied to our data set, both criteria yielded the same results with the exception of one TF muscle synergy in two subjects. To ensure that $N_{syn\text{-}S}$ or $N_{syn\text{-}T}$ was appro-

priately determined, we also validated $N_{syn\text{-}S}$ and $N_{syn\text{-}T}$, using factor analysis (FA). One to ten factors were extracted, and likelihood ratios were computed for the addition of another muscle synergy. We then graphed the log likelihood versus number of factors; $N_{syn\text{-}S}$ and $N_{syn\text{-}T}$ were chosen as the point on the log likelihood plot that had the greatest curvature (Tresch et al. 2006). For SF muscle synergies, if there was a discrepancy between $N_{syn\text{-}S}$ calculated from VAF versus FA, we examined the spatial tuning curves of the SF muscle synergies themselves. If the addition of a muscle synergy yielded a flat or nondescript tuning curve, the additional SF muscle synergy was likely accounting for noise and was not included in analysis. For TF muscle synergies, there was no discrepancy between $N_{syn\text{-}T}$ with either VAF or FA.

For both SF and TF muscle synergies, we estimated the VAF confidence interval (CI) for each muscle synergy extraction and ensured that the VAF CIs were nonoverlapping compared with SF or TF muscle synergies extracted from a shuffled matrix of the same data (Cheung et al. 2009). Each muscle was shuffled independently, yielding the same values, range, and variance for muscles with different intermuscular relationships. The 95% CI for VAF was estimated with bootstrapping. All actual and shuffled data sets were resampled 500 times with data replacement, and VAF was calculated from each resampling. VAF values were then ordered; the 95% CI was represented as the 2.5 and 97.5 percentiles of VAF distribution.

### *Muscle Synergy Analysis*

We compared the degree to which SF or TF muscle synergy extractions could account for total and muscle VAF. We performed a three-way ANOVA (subject × extraction method × data set) on total and muscle VAF for SF and TF muscle synergies, using both actual and shuffled data sets (Zar 1999). We then verified the level of significance between groups, using Tukey-Kramer post hoc tests ($\alpha = 0.01$).

SF and TF muscle synergies were used to reconstruct EMG patterns for all perturbations. Measured and reconstructed data were compared over trials, muscles, and perturbation directions to quantify the ability of SF versus TF muscle synergies to faithfully reproduce EMG activity throughout perturbations in all subjects. We used $r^2$ and VAF to quantify the similarity between measured and reconstructed EMG (Torres-Oviedo et al. 2006; Zar 1999). Both centered ($r^2$) and uncentered (VAF) Pearson correlations were necessary: $r^2$ is high when shapes but not amplitudes of EMG traces are well matched, while VAF is high when amplitude is high but shapes of traces are noisy.

We further determined the structural consistency of SF muscle synergies across different epochs of perturbations by calculating correlation coefficients ($r$) between pairs of SF muscle synergies. SF muscle synergies from individual epochs were paired with SF muscle synergies from all epochs pooled together that yielded the highest value of $r$; this criterion ensured that only positive correlations between SF muscle synergies were considered. We considered a pair of SF muscle synergies to have consistent structure if $r > 0.623$, which corresponds to the critical value of $r^2$ for 16 elements at $P = 0.01$ ($r^2 = 0.388$). However, because the NNMF algorithm constrains muscle synergies to be nonnegative, we expected positive correlations by chance. Therefore, we generated 25,000 random permutations of the elements of SF muscle synergies extracted from the entire perturbation for each subject, yielding a distribution of chance $r$ values with an expected mean ($\mu$) and standard deviation ($\sigma$) (Berniker et al. 2009). An $r$-value of 0.623 corresponded to the 99th percentile of the distribution ($P = 0.008$). Therefore, SF muscle synergy comparisons with $r > 0.623$ were considered more similar than expected by chance; comparisons with $r \leq 0.623$ were considered uncorrelated and labeled as "additional."

### *Feedback Model*

To test our hypothesis that SF muscle synergies have time-varying recruitment patterns that are modulated by temporal feedback patterns, we fit SF muscle synergy recruitment patterns in anterior and posterior directions by using a "jigsaw" model based on delayed feedback of CoM kinematics as in previous studies (Welch and Ting 2009) (Fig. 3). The model assumes that CoM kinematic signals are linearly combined to recruit SF muscle synergies in a feedback manner. Using CoM horizontal displacement (**d**), velocity (**v**), and acceleration (**a**), we reconstructed recruitment patterns **C** for each SF muscle synergy $\mathbf{W}_i$ ($\mathbf{C}_{W_i}$) by assigning feedback gains ($k_d$, $k_v$, $k_a$) at a common time delay ($\lambda$), representing neural transmission and processing time, and then half-wave rectifying the muscle synergy recruitment pattern found, using the equation below:

$$\mathbf{C}_{W_i} = k_d\mathbf{d}(t-\lambda) + k_v\mathbf{v}(t-\lambda) + k_a\mathbf{a}(t-\lambda)$$

Muscle synergies extracted from pooled perturbation epochs were used to reconstruct EMG activity throughout all A-P trials, yielding

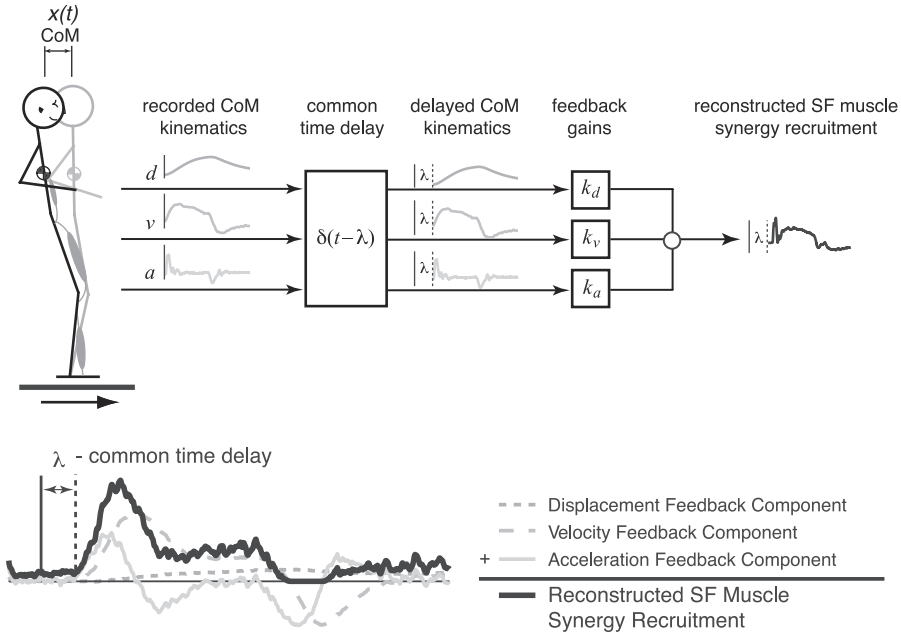


Fig. 3. Delayed feedback model. Recorded CoM kinematics from anterior-posterior (A-P) perturbations are used to reconstruct SF muscle synergy recruitment patterns throughout a perturbation. Each component of CoM motion is multiplied by a feedback gain at a common time delay and linearly added to produce a reconstructed SF muscle synergy recruitment pattern.

temporal recruitment patterns. The recruitment patterns were then interpolated and resampled at 1,000 Hz for finer resolution. For every A-P trial, all active muscle synergies were included in analysis; an active muscle synergy was defined as a muscle synergy that was recruited at ≥20% of maximum activation (determined over all trials) for at least 30 ms. All analyses were performed over a 1-s time interval, beginning 100 ms before platform onset ($t = 0$) to the end of the *stable* epoch of EMG activity following the end of the perturbation ($t_{end}$; 900 ms after perturbation onset). The initial feedback gains $k_i$ were constrained to be between −5 and 5; this range was about an order of magnitude larger than the range of typical feedback gain values. The time delay λ was restricted to be between 90 and 150 ms, a range encompassing physiological delays of muscle activity to postural responses (Horak and Macpherson 1996). For each muscle synergy, three feedback gains ($k_i$) and a common time delay (λ) were identified that best reproduced the SF muscle synergy recruitment patterns according to the cost function

$$\min\left\{\mu_s\int_0^{t_{end}} e_m^2 dt + \mu_k \max(|e_m|)\right\}$$

The first term penalized the squared error ($e_m$) between recorded and simulated muscle synergy recruitment patterns throughout the perturbation with weight $\mu_s$. The second term penalized maximum error between simulated and recorded data at any point in time with weight $\mu_k$. The ratio of $\mu_s$ to $\mu_k$ was 10:1. Temporal patterns of recruitment for each SF muscle synergy were determined independently, yielding an independent set of feedback gains in response to the same CoM kinematics for a given trial. Feedback gains were then averaged over all trials and used to reconstruct SF muscle synergy recruitment patterns for active muscle synergies.

We also quantified the similarity between SF muscle synergy recruitment patterns obtained from experimental data and those reconstructed from the delayed feedback model. Recruitment patterns were considered well-reconstructed when mean $r^2 \geq 0.5$ or mean VAF ≥ 75% for all trials in an active SF muscle synergy. The reconstructed SF muscle synergy recruitment patterns were also used to reconstruct observed EMG throughout A-P perturbations; $r^2$ and VAF were used to quantify the similarity between recorded and reconstructed EMG.

## RESULTS

### *Summary*

For each subject, a small number of both SF and TF muscle synergies was able to explain the majority of the variability in muscle activity throughout the time course of postural responses to perturbations. A small number of SF muscle synergies (≤7) accounted for significantly more EMG variability than a small number of TF muscle synergies. In each subject, a consistent set of SF muscle synergies was found across different epochs of postural responses. Furthermore, in anterior and posterior perturbations, SF muscle synergies exhibited variable recruitment patterns across trials, which were sufficient to explain differences in EMG patterns across trials and in different perturbation epochs. Temporal patterns of SF muscle synergy recruitment in anterior and posterior perturbations were well-reconstructed by delayed feedback of CoM kinematics in all subjects. Trial-by-trial variations in SF muscle synergy recruitment patterns were accounted for by trial-by-trial differences in CoM kinematics and a fixed set of feedback gains ($k_d$, $k_v$, $k_a$). Thus EMG patterns measured throughout A-P perturbations could be reconstructed by a low-dimensional delayed feedback model that recruits SF muscle synergies based on CoM kinematics.

### *Postural Responses Throughout Perturbations*

CoM kinematics and intermuscular coordination patterns differed across perturbation epochs in postural responses to ramp-and-hold perturbations (Fig. 2). During the *start* epoch, CoM kinematic vectors (**d**, **v**, **a**) were all oriented in the same direction, opposite that of platform acceleration. During the *stop* epoch, the platform decelerated to a final position, such that the resulting CoM acceleration vector was opposite the direction of platform acceleration as well as opposite to the CoM position and velocity vectors (Fig. 2). Similarly, some muscles (e.g., ERSP, SEMT) had bursts mainly in the *start* epoch in a manner resembling CoM acceleration. Other muscles (e.g., VMED) showed increased activity later in the perturbation, similar to CoM displacement. Another subset of muscles (e.g., TA) showed an initial burst of activity followed by sustained activity throughout the perturbation. In addition, some muscles exhibited large bursts of activity at inconsistent times during the postural response; these were largely proximal muscles that moved the trunk, consistent with the "hip" strategy. These types of responses were seen over all perturbation directions for all subjects.

### *EMG Reconstructions Using SF Versus TF Muscle Synergies*

We quantified the ability of SF versus TF muscle synergies to reconstruct EMG variability (VAF) throughout a postural task. However, because SF versus TF muscle synergy analyses impose different constraints, we evaluated EMG reconstructions of SF versus TF muscle synergies in three ways to avoid biasing results toward either an SF or a TF muscle synergy organization. We first quantified total and muscle VAF, using previously established criteria for the number of SF muscle synergies ($N_{syn\text{-}S}$). We then compared total VAF, muscle VAF, and individual EMG reconstructions using $N_{syn\text{-}S}$ SF muscle synergies to reconstructions using different numbers of TF muscle synergies found by *1*) previously established criteria for identifying TF muscle synergies ($N_{syn\text{-}T}$), *2*) using the same number of components as SF muscle synergies ($N_{syn\text{-}S}$), and *3*) roughly matching the total number of parameters present in the model with $N_{syn\text{-}S}$ SF muscle synergies ($N_{syn\text{-}P}$).

SF muscle synergies reproduced postural EMG variability better than TF muscle synergies using either similar criteria or the same number of components (Fig. 4*A*). Across all subjects, more SF muscle synergies ($N_{syn\text{-}S}$: 5–7) were identified compared with TF muscle synergies ($N_{syn\text{-}T}$: 2–4). $N_{syn\text{-}S}$ SF muscle synergies accounted for significantly more total VAF than $N_{syn\text{-}T}$ TF muscle synergies across all subjects (Fig. 4*A*; $N_{syn\text{-}S}$ total VAF = 85–92%, mean VAF ± SD = 88 ± 2%; $N_{syn\text{-}T}$ total VAF = 75–85%, mean VAF ± SD = 79 ± 3%; $F[3,63] = 81.57$, $P < 10^{-16}$; $P < 0.01$ by Tukey-Kramer post hoc analysis). Moreover, $N_{syn\text{-}S}$ SF muscle synergies accounted for more muscle VAF than $N_{syn\text{-}T}$ TF muscle synergies in all subjects at $\alpha = 0.01$ ($N_{syn\text{-}S}$ muscle VAF = 31–100%, 85 ± 13%; $N_{syn\text{-}T}$ muscle VAF = 75–85%, 79 ± 3%; $F[3,1023] = 79.25$; $P < 10^{-16}$; $P < 0.01$ by Tukey-Kramer post hoc analysis). To ensure that the observed differences in VAF were not due to the smaller number of TF muscle synergies, we quantified VAF using $N_{syn\text{-}S}$ TF muscle synergies. The total VAF of the data set using $N_{syn\text{-}S}$ TF muscle synergies was still significantly lower than that of $N_{syn\text{-}S}$ SF muscle synergies (Fig. 4*A*; $N_{syn\text{-}S}$ TF VAF = 85 ± 2%; $P < 0.01$).

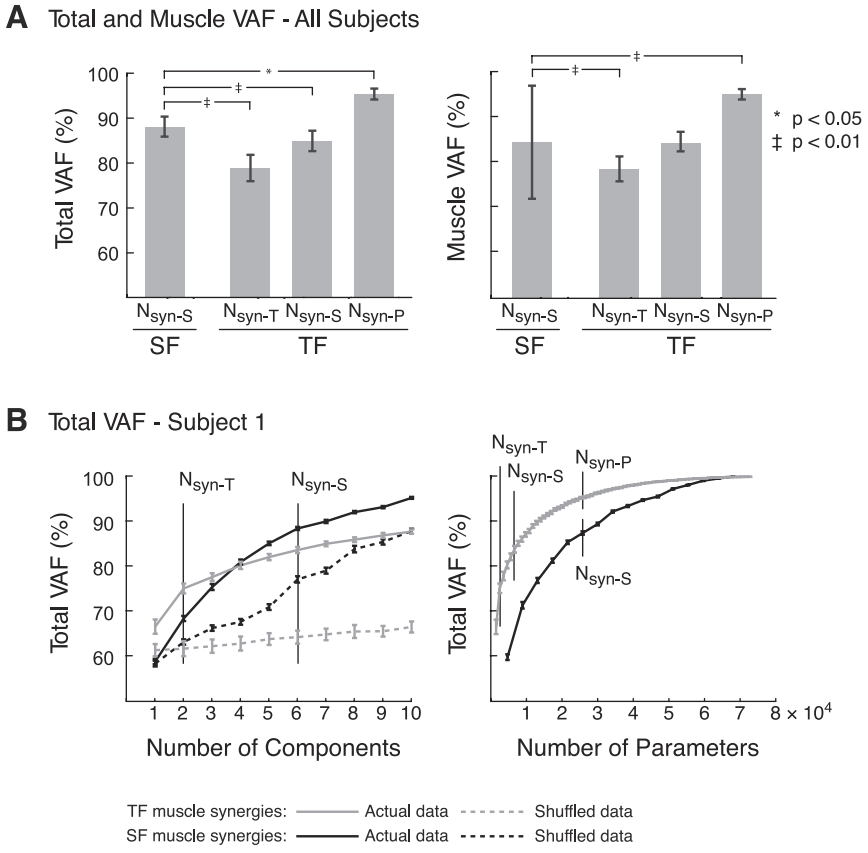


Fig. 4. Variability accounted for (VAF) comparisons using TF vs. SF muscle synergies. *A*: total and muscle VAF for all subjects. $N_{syn\text{-}S}$ SF muscle synergies explain a significantly larger portion of the data set than $N_{syn\text{-}T}$ or $N_{syn\text{-}S}$ TF muscle synergies but significantly less variability than $N_{syn\text{-}P}$ TF muscle synergies. Error bars represent SD. $^*P < 0.05$, $‡P < 0.01$, ANOVA, Tukey-Kramer post hoc tests. *B*: total VAF for *subject 1*. *Left*: total VAF vs. number of components. Total VAF with $N_{syn\text{-}S}$ SF muscle synergies is higher than VAF with $N_{syn\text{-}T}$ or $N_{syn\text{-}S}$ TF muscle synergies. Both methods of synergy extraction account for significantly more variability than with shuffled muscle synergies. *Right*: total VAF vs. number of parameters incorporated into the muscle synergy extraction. VAF of TF muscle synergies was always higher than SF muscle synergies. However, many more TF muscle synergies (25) were needed to incorporate the same number of parameters as SF muscle synergies (6). Error bars represent the estimated 95% confidence interval of VAF.

We also evaluated EMG reconstructions using SF versus TF muscle synergies to match the total number of parameters present in the two methods of analysis ($N_{syn\text{-}P}$ TF vs. $N_{syn\text{-}S}$ SF muscle synergies). A much larger number of TF muscle synergies was necessary ($N_{syn\text{-}P}$: 20–29) in order to incorporate roughly the same number of parameters for TF and SF muscle synergy extractions. However, with $N_{syn\text{-}P}$ TF muscle synergies, both total VAF and muscle VAF were significantly higher than with $N_{syn\text{-}S}$ SF muscle synergies (Fig. 4*A*; $N_{syn\text{-}P}$ TF total VAF $= 95 \pm 1\%$, $P < 0.05$; $N_{syn\text{-}P}$ TF muscle VAF $= 95 \pm 1\%$, $P < 0.01$).

The differences in total VAF between SF and TF muscle synergies were found in each subject. For example, in a representative subject (*subject 1*), six SF muscle synergies were needed to meet the criteria for EMG reconstruction. By contrast, only two TF muscle synergies were needed to meet the criteria (Fig. 4*B*, *left*). On average, the lower limit of the 95% CI for total VAF of $N_{syn\text{-}S}$ SF muscle synergies was 4.0 CIs higher than the upper limit of the 95% CI for $N_{syn\text{-}T}$ TF muscle synergies. In our representative subject, the lower limit of the 95% CI for total VAF of $N_{syn\text{-}S}$ SF muscle synergies was 1.8 CIs higher than the upper limit of the 95% CI for $N_{syn\text{-}S}$ TF muscle synergies (Fig. 4*B*). When comparing VAF as a function of the number of parameters, VAF was always higher for TF versus SF muscle synergies (Fig. 4*B*, *right*). However, 25 TF muscle synergies were needed to incorporate the same number of parameters as $N_{syn\text{-}S}$ SF muscle synergies.

SF muscle synergy structure was different from TF muscle synergy structure, and TF muscle synergy structure varied depending on the criteria used (Fig. 5*A*). Because SF muscle synergies fractionated muscle activity spatially, each SF muscle synergy corresponded to a specific muscle coordination pattern. Note that muscles with multiple actions (i.e., RFEM) can belong to more than one SF muscle synergy with presumably different functions (e.g., W4: RFEM/TA; W6: RFEM/quadriceps). Moreover, antagonistic muscles such as TA and MGAS are not grouped in the same SF muscle synergy. In contrast, TF muscle synergies fractionated muscle activity by time (Fig. 5*A*, *right*). Each TF muscle synergy was activated in a localized region in time; this time-localized region became shorter and shorter as the number of TF muscle synergies increased.

Individual muscle reconstructions were fundamentally different when using SF versus TF muscle synergies (Fig. 5*B*). For example, in individual muscle reconstructions for a forward-leftward (150°) perturbation using SF muscle synergies, RFEM was reconstructed with W4 and W6. Moreover, antagonistic muscles TA and MGAS were reconstructed with different SF muscle synergies W4 and W2, respectively (Fig. 5*B*, *left*). In contrast, regardless of the number of components used, the majority of TF muscle synergies were used to reconstruct any one muscle. For example, both C1 and C2 were used to reconstruct RFEM as well as antagonistic muscles TA and MGAS when using $N_{syn\text{-}T}$ TF muscle synergy components (Fig. 5*B*). Although muscle reconstructions improved when using $N_{syn\text{-}S}$ or $N_{syn\text{-}P}$ TF muscle synergies, a majority of TF muscle synergies were still used to reconstruct all muscles. Moreover, the increased localization of the TF muscle synergies approached the time resolution of the EMG signals.

When reconstructing EMG data across perturbation directions, SF muscle synergies had more consistent temporal recruitments than the spatial weightings of TF muscle synergies

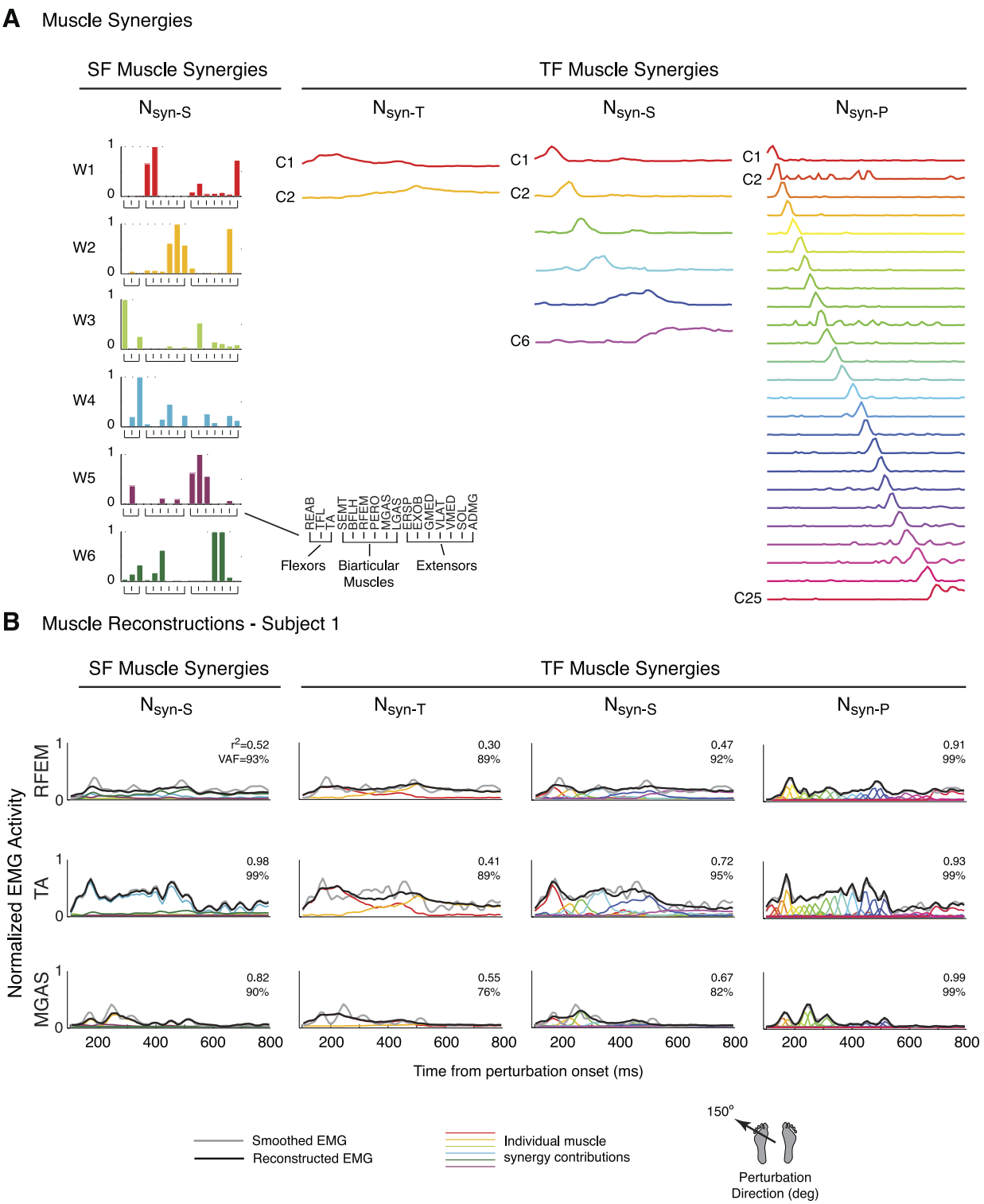


Fig. 5. Comparison of SF vs. TF muscle synergy structure and muscle reconstructions. *A*: muscle synergy structure. SF muscle synergies organize muscle activity into groups of muscles that have common spatial activation patterns (*left*). TF muscle synergies organize muscle activity into consistent temporal patterns (*right*). As the number of TF muscle synergies increases, temporal patterns of activation become more localized in time. Data are shown for *subject 1*. *B*: muscle reconstructions during a forward-leftward (150°) perturbation. A small subset of SF muscle synergies was recruited to reconstruct each muscle (*left*). Note that multiple SF muscle synergies contributed to the reconstruction of muscles with multiple actions [i.e., W4 and W6 for rectus femoris (RFEM)], and separate SF muscle synergies were recruited in antagonistic muscle pairs [W4 for TA, W2 for medial gastrocnemius (MGAS)]. In contrast, a majority of TF muscle synergies was recruited to reconstruct each muscle (*right*). The same TF muscle synergies were used to recruit antagonistic muscle pairs. Gray lines, smoothed EMG; black lines, reconstructed EMG; colored lines, individual muscle synergy contributions. REAB, rectus abdominus; TFL, tensor fascia lata; BFLH, biceps femoris, long head; PERO, peroneus; LGAS, lateral gastrocnemius; EXOB, external oblique; GMED, gluteus medius; VLAT, vastus lateralis; SOL, soleus; ADMG, adductor magnus.

(Fig. 6). Because muscle activity is tuned to certain spatial directions, SF muscle synergies are recruited only in a subset of directions. For example, in *subject 1* W2 comprising mainly calf muscles had large temporal patterns of recruitment in backward and backward-leftward perturbations (210–300°) that caused dorsiflexion (Fig. 6*A*). Although TF muscle synergies are recruited across all perturbation directions, the muscle weightings varied considerably. TF muscle synergy C1 was mainly active in the initial postural response (Fig. 6*B*), activating mainly TA in forward-rightward perturbations (0–60°), TA with proximal muscles (EXOB, GMED, TFL) in forward-leftward perturbations (120–180°), and TA with calf muscles (PERO, MGAS, LGAS, SOL) in backward-leftward perturbations (210–270°). Because a single TF muscle synergy describes the muscle activity of a small time bin, the resulting muscle weightings describe the EMG pattern during that time bin.

### *SF Muscle Synergies Have Similar Structure Across Perturbation Epochs*

A small number of SF muscle synergies independently extracted from different perturbation epochs could equally explain the total EMG variability of postural responses. Only 3–7 SF muscle synergies were necessary to reconstruct the activity of 16 muscles during postural perturbations in all subjects, regardless of the extraction epoch (cf. Fig. 2). Four to six SF muscle synergies accounted for EMG activity in *start* (total VAF = 87 ± 2%) and *plateau* (86 ± 4%) epochs, consistent with previous studies on human balance (Torres-Oviedo and Ting 2007). In addition, three to six SF muscle

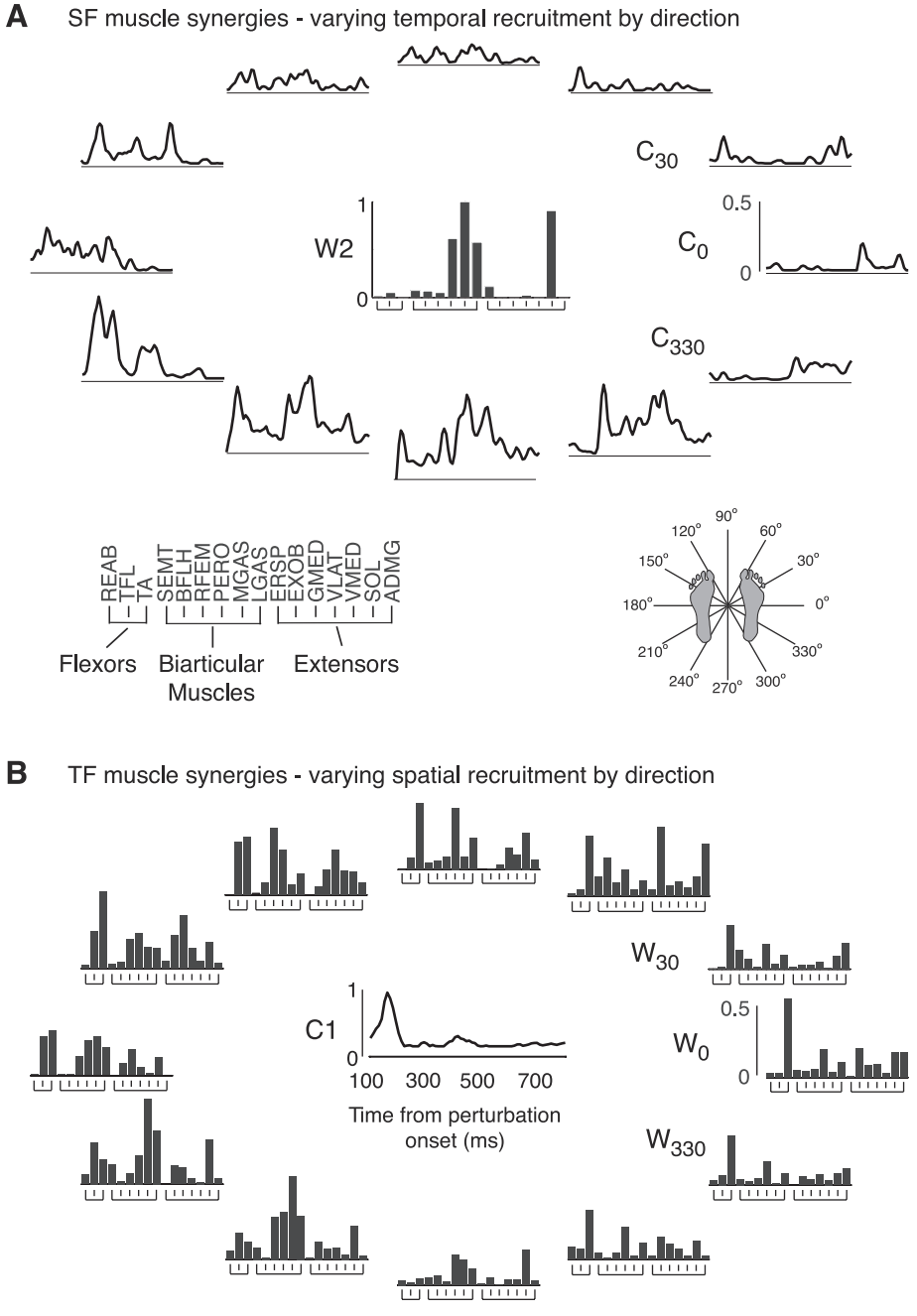


Fig. 6. Variable SF muscle synergy recruitment vs. variable TF muscle synergy weighting across multidirectional perturbations. *A*: SF muscle synergies. SF muscle synergy recruitment was variable over directions but consistently recruited in backward and leftward (210–300°) perturbations. *B*: TF muscle synergies. TF muscle synergy weightings changed considerably over directions and trials and included antagonistic pairs of muscles. Data are shown for the same subject as in Fig. 5 (*subject 1*).

synergies were able to account for EMG activity in previously unexamined *stop* (88 ± 4%) and *stable* (88 ± 1%) epochs with 10-ms bins. Five to seven SF muscle synergies were necessary to reproduce EMG activity from the entire perturbation (87 ± 3%).

In all subjects, a subset of SF muscle synergies extracted from individual epochs had consistent structure compared with SF muscle synergies extracted from the entire perturbation. Two to four SF muscle synergies per subject were consistent across all epochs at $P < 0.01$ ($0.62 \leq r \leq 1.0$; $r = 0.88 \pm 0.10$). Moreover, one to five SF muscle synergies per subject were not identified in every epoch but were consistent whenever they were found ($0.66 \leq r \leq 1.0$, $r = 0.90 \pm 0.10$). Six of eight subjects had at least one additional SF muscle synergy; these SF muscle synergies were most often found in the *start* and *plateau* epochs and were most often composed of proximal muscles that acted at the hip joint.

The level of consistency in SF muscle synergy structure across epochs was robust for all subjects. For example, *subject 7* had the highest comparisons between SF muscle synergy pairs (Fig. 7*A*). In *subject 7*, four of the six SF muscle synergies (W1, W2, W3, W6) were consistent across every epoch ($0.76 \leq r \leq 1.0$, $r = 0.92 \pm 0.073$). W4 and W5 were consistent across epochs where they were identified ($0.68 \leq r \leq 0.99$, $r = 0.90 \pm 0.15$). *Subject 5* had the lowest level of consistency between SF muscle synergy pairs (Fig. 7*B*). For *subject 5*, all six SF muscle synergies from the entire perturbation (*all*) had consistent structure with SF muscle synergies from various epochs ($0.67 \leq r \leq 0.99$, $r = 0.86 \pm 0.10$). However, three additional SF muscle synergies (W7, W8, W9) were identified. Of the additional SF muscle synergies, W7 was composed primarily of ankle flexors TA and PERO, W8 consisted mainly of RFEM, a biarticular muscle that aids in hip flexion, and W9 was composed mainly of hamstring muscles (BFLH, SEMT) as well as muscles that act at the hip and trunk (EXOB, ERSP, GMED).

### *Consistent SF Muscle Synergies Across Subjects*

Although different subjects had different numbers of SF muscle synergies, the muscular composition of SF muscle synergies was similar across subjects (Fig. 8). Ten different SF muscle synergies were found across all subjects. Two SF muscle synergies (W2, W6) were found in all eight subjects ($0.71 \leq r \leq 0.96$, $r = 0.87 \pm 0.072$) and had muscles spanning the ankle and knee, respectively. Three additional SF muscle synergies (W1, W2, W5) were found in seven of eight subjects ($0.62 \leq r \leq 0.95$, $r = 0.83 \pm 0.11$), having actions of hamstring and trunk muscles. Three of the remaining four SF muscle synergies (W4, W7, W8) were found in only two to four subjects; W4 was composed mainly of calf muscles, W7 of hip muscles, and W8 of hamstrings. Two SF muscle synergies (W9 and W10) were statistically different from all of the other SF muscle synergies and had a large hamstring or trunk muscle contribution.

### *CoM Kinematic Feedback Reconstructs SF Muscle Synergy Recruitment*

SF muscle synergies exhibited time-varying recruitment patterns across directions with considerable trial-to-trial variability (Fig. 9). For each perturbation direction, a subset of SF muscle synergies was recruited to maintain balance. Each SF muscle synergy was recruited in response to a subset of perturbation directions. For example, data from a representative subject (*subject 2*) are shown for one forward and one backward trial (Fig. 9*A*). In this subject, four muscle synergies (W1, W3, W4, W6) were active (recruited at ≥20% of maximum activity for at least 30 ms) in forward (90°) perturbations; W2 and W5 were active in backward (270°) perturbations. In contrast, W4 was active in mediolateral (0°/180°) perturbations. Within a given perturbation direction, active SF muscle synergies were recruited at different times during the perturbation. For forward perturbations, W1, W5, and W6 had bursts of activity in the *start* epoch. While W6 was mainly active during the *start* epoch alone, W1 and W5 had continued activity extending through the *stop* epoch. W5 remained active during the *stable* epoch. W3 was active in the *plateau* through *stable* epochs, peaking during the *stop* epoch. For backward perturbations, W2 was active in the *start* and *plateau* epochs. W5 was active during the *start* epoch. SF muscle synergy recruitment patterns also varied from trial to trial; for example, W1 was recruited differently across five anterior perturbations (Fig. 9*B*).

For each subject, a subset (2–7) of active SF muscle synergy recruitment patterns was well reconstructed in A-P perturbations. We only considered the recruitment of active SF muscle synergies, which had ≥20% of maximum activity for at least 30 ms in a trial. In a subject representative of our average results (*subject 2*), four of five SF muscle synergies (W1, W2, W5, W6) were well-reconstructed (Fig. 9*A*). While W5 was also defined as active in the backward direction by our criteria, it was not well-reconstructed for backward perturbations (Fig. 9*A*). We defined a well-reconstructed SF muscle synergy recruitment pattern to have an average $r^2 \geq 0.50$ or VAF ≥ 75% over all trials. This threshold was well above the reconstruction of SF muscle synergy recruitment patterns using shuffled CoM kinematics ($r^2 = 0.02 \pm 0.027$; VAF = 31 ± 16%). W1 responded similarly to backward position, velocity, and acceleration, W2 responded mainly to forward velocity, W5 responded mainly to backward position, and W6 responded mainly to backward acceleration. Time delays were between 100 and 120 ms for all trials, consistent with postural delays described in the literature. Although the feedback model reconstructed most of the contour of the recruitment patterns, it often did not account for short bursts in the *start* epoch of individual trials (data not shown). However, these short bursts were seen in perturbations of many directions and likely represented cocontraction of muscles in response to the onset of perturbation.

With the feedback model, a fixed set of feedback gains ($k_d$, $k_v$, $k_a$) could reconstruct trial-by-trial variability in SF muscle synergy recruitment patterns (Fig. 9*B*) but could not account for the time course of TF muscle synergies. While W1 was recruited differently over all five forward perturbations, the differences in W1 recruitment could be reconstructed by the differences in CoM kinematics for each trial. For example, CoM velocity peaked twice in *trials 4* and *5*; these peaks were seen in the actual and reconstructed recruitment of W1 for these trials. Similarly, CoM displacement remained high throughout *trials 1* and *4*, resulting in continued W1 recruitment (actual and reconstructed) in the *stable* epoch for these trials. While CoM feedback on SF muscle synergies did not predict all bursts in SF

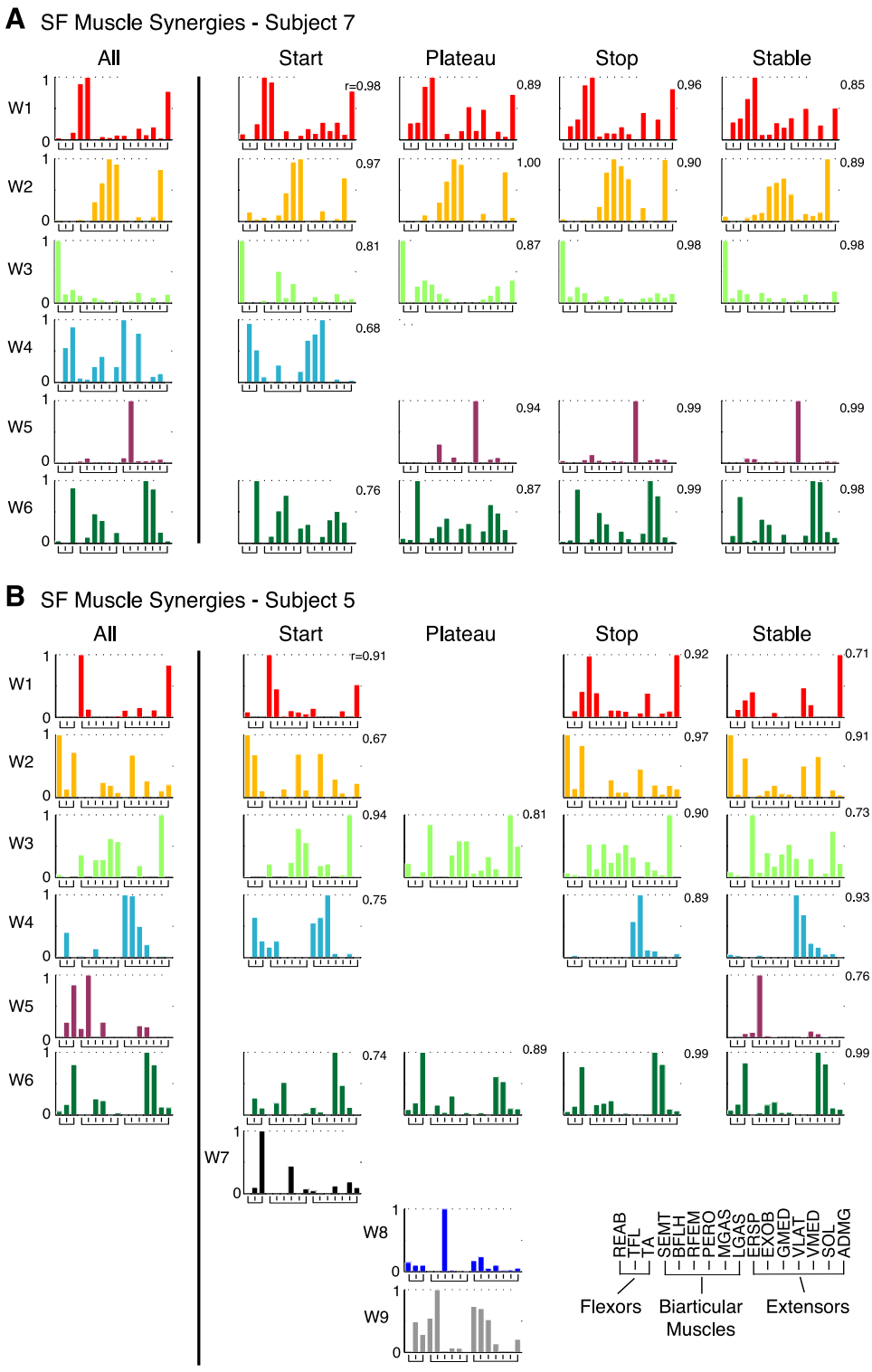


Fig. 7. Comparison of SF muscle synergy structure across various epochs throughout a perturbation. *A*: comparisons for a subject with high structural consistency (*subject 7*). SF muscle synergies extracted independently from *start*, *plateau*, *stop*, and *stable* epochs were similar to those extracted from all epochs pooled together (*all*). W1, W2, W3, and W6 were identified in every epoch, while W4 and W5 were only identified in some epochs. *B*: comparisons for a subject with low structural consistency (*subject 5*). W3 and W6 were identified in every epoch, while W1, W2, W4, and W5 were only identified in some epochs. Three SF muscle synergies were uncorrelated at $P < 0.01$ ($r < 0.623$) and were considered "additional." W7 was mainly composed of ankle muscles TA and PERO, W8 was mainly composed of RFEM, a biarticular muscle that aids in hip flexion, and W9 had large involvement of hamstrings (BFLH, SEMT) and muscles with actions at the trunk and hip (EXOB, ERSP, GMED).

muscle synergy recruitment (e.g., *stop* and *stable* epochs in *trial 2*), CoM feedback on TF muscle synergies could not account for any trial-by-trial variability, as the temporal commands were fixed across trials for a given time epoch by definition. Furthermore, a given TF muscle synergy exhibited the same pattern of recruitment for all directions of perturbation, resulting in inconsistent feedback gains for every direction of perturbation.

A delayed feedback model based on CoM kinematics reproduced a majority of SF muscle synergy recruitment patterns throughout A-P perturbations across all subjects. Across all subjects, the recruitment patterns of 34 of 44 SF muscle synergies were well reconstructed by the feedback model (Fig. 8). For all SF muscle synergies, the model used a delay ($\lambda$) of 100–130 ms, consistent with previously described postural delays (Horak and Macpherson 1996; Nashner

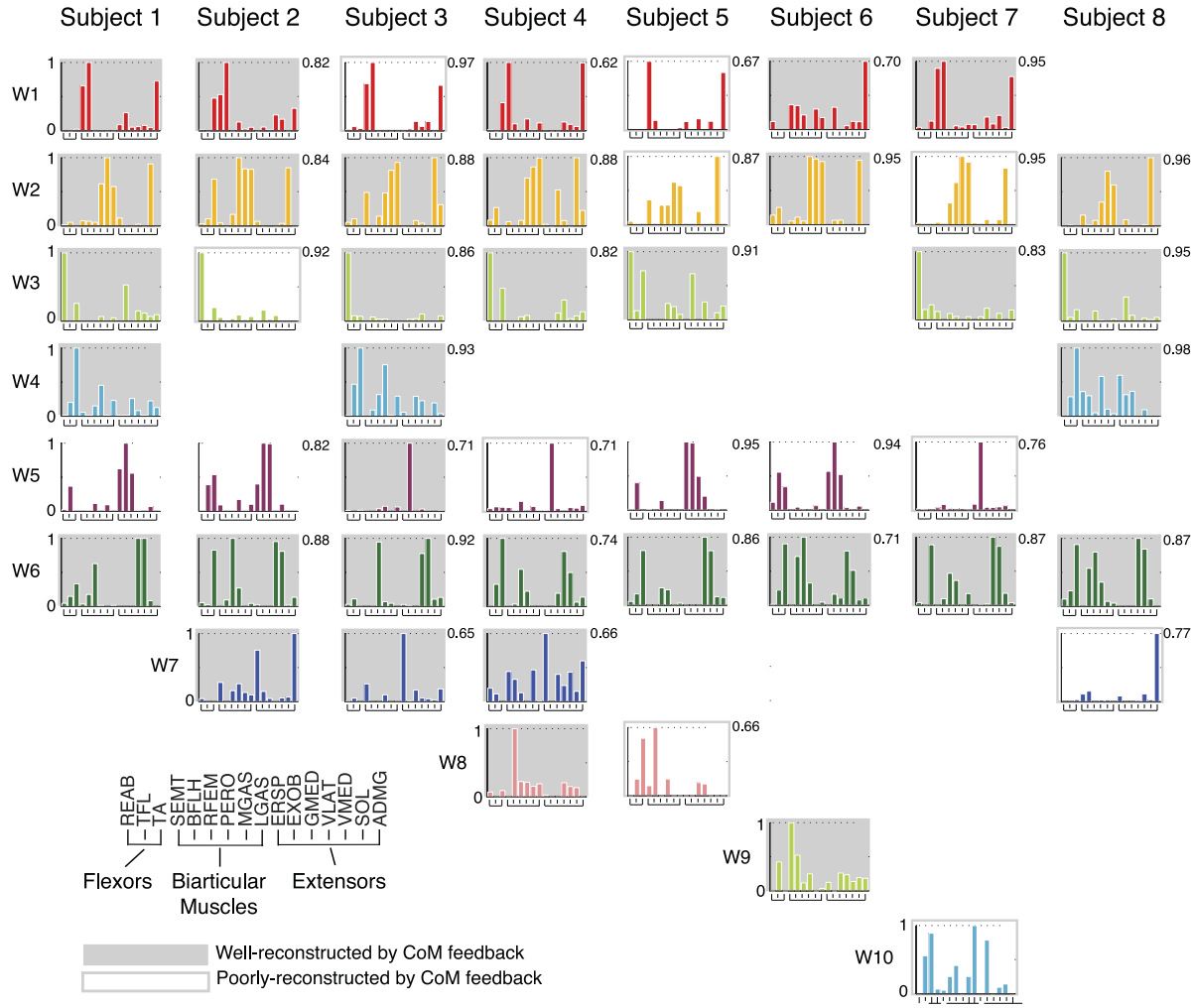


Fig. 8. SF muscle synergies extracted from the entire time course of perturbations for all subjects. Five of 10 SF muscle synergies (W1, W2, W3, W5, W6) were similar in at least 7 of 8 subjects. Of the remaining SF muscle synergies, W8 and W9 had large contributions from the hamstrings (BFLH, SEMT), biarticular muscles that aid in hip extension. W10 had large contributions from trunk muscles. Gray shaded and outlined SF muscle synergies were active during A-P perturbations ($n = 44$). For active SF muscle synergies, shaded muscle synergies were well-reconstructed with a delayed feedback model based on CoM motion across A-P trials (34/44). Outlined muscle synergies (10/44) were poorly reconstructed by the feedback model. Of these 10 SF muscle synergies, 6 had major contribution of mono- and biarticular muscles acting at the hip. Numbers indicate $r$ values for comparisons.

1976). Ten of the forty-four SF muscle synergies across subjects were poorly reconstructed by the feedback model in A-P perturbations (Fig. 8). These SF muscle synergies had unpredictable and/or inconsistent recruitment patterns (e.g., Fig. 9*A*, W3). Eight of the ten poorly constructed SF muscle synergies involved hip and hamstring muscles. Two more poorly reconstructed SF muscle synergies had a major contribution of RFEM, a biarticular muscle that aids in hip flexion. In addition, two subjects had SF muscle synergies with inconsistent feedback gains between A-P perturbations (4 SF muscle synergies total). These SF muscle synergies also had large contribution of mono- and biarticular muscles that act at the hip. To determine whether hip angle kinematics could be responsible for SF muscle synergy recruitment patterns in the poorly reconstructed SF muscle synergies, we qualitatively compared the hip angle kinematics to muscle synergy recruitment. While the hip angle kinematics were different from CoM kinematics, changes in hip kinematics were not seen until after the onset of SF muscle synergy recruitment patterns, making hip angle kinematics an unlikely candidate for driving the recruitment of SF muscle synergies with actions at the hip.

### *SF Muscle Synergies Recruited by CoM Feedback Reproduce Temporal Variations in Muscle Activity*

By flexibly combining SF muscle synergies with time-varying recruitment patterns, a small set of SF muscle synergies reconstructed muscle activity throughout postural responses to A-P perturbations (Fig. 10, *left*). Of 16 surface EMGs, 5–7 SF muscle synergies were needed to reproduce muscle activation patterns in all subjects. These SF muscle synergies were able to reproduce bursts of activity seen in *start* and *stop* epochs, as well as continuing muscle activity seen in *plateau* and *stable* epochs for all A-P trials ($r^2 = 0.78 \pm 0.16$; VAF $= 91 \pm 9\%$). It should be noted that the recruitment patterns of individual SF muscle synergies (colored lines in Fig. 10) were scaled differently for each muscle; the scaling corresponds to the muscular contribution of each SF muscle synergy (see Fig. 9, muscle synergy composition and recruitment). Also note that multiple SF muscle synergies can con-

tribute to a temporal EMG pattern. For example, in forward perturbations, EMG activity of ADMG during the *start* epoch is mainly reconstructed with W6 (blue). In the late *plateau* and *stop* epochs, W1 (red) is the major contributor to ADMG activity. Similarly, the initial burst of PERO in backward perturbations is reconstructed with W2 (orange) with a contribution of W6 (blue) to reconstruct later activity.

Feedback model reconstructions of SF muscle synergy recruitment patterns were also able to reconstruct muscle activity throughout postural responses to perturbations (Fig. 10, *right*). By replacing SF muscle synergy recruitment patterns determined by NNMF with feedback model recruitment patterns, EMG activity was reconstructed throughout A-P perturbations in all trials for all subjects ($r^2 = 0.65 \pm 0.22$; VAF = 85 ± 11%). However, correlation values were significantly lower than those for EMG reconstructed from NNMF recruitment patterns ($P < 0.01$ for $r^2$ and VAF). This discrepancy may be due to the low-frequency signal of feedback model recruitment patterns being unable to reproduce higher-frequency oscillations seen in EMG patterns. Alternatively, high-frequency oscillations in SF muscle synergy recruitment patterns may represent high-frequency coupling of muscles due to either a slightly different form of feedback or the superposition of CoM feedback with other concurrent feedback mechanisms. Nevertheless, $N_{syn\text{-}S}$ SF muscle synergies with feedback model recruitment patterns still reconstructed EMG activity significantly better than TF muscle synergies in all subjects with either $N_{syn\text{-}T}$ ($r^2 = 0.35 \pm 0.17$; VAF = 78 ± 11%; $P < 0.01$ for $r^2$ and VAF) or $N_{syn\text{-}S}$ ($r^2 = 0.51 \pm 0.17$; VAF = 84 ± 8%; $P < 0.01$ for $r^2$) TF muscle synergies.

## DISCUSSION

### *Summary*

Taken together, our results suggest that the nervous system produces motor outputs by using a multisensory estimate of task-level variables to modulate SF muscle synergies. SF muscle synergies provide a low-dimensional sensorimotor transformation whereby task-level variables can be mapped to execution-level variables that define the spatiotemporal patterns of muscles. For standing balance control, many of the identified SF muscle synergies were recruited throughout postural perturbations by delayed feedback on the task-level variables defined by CoM kinematics. Thus the low-dimensional organizations of the temporal and spatial features of muscle coordination are independent during postural responses to perturbations. These results are consistent with a hierarchical neural control scheme in which a low-dimensional feedback structure recruits SF muscle synergies.

### *Feedback Control of SF Muscle Synergies for Standing Balance*

Our results support the idea that the temporal modulation of SF muscle synergies is a general neural mechanism for producing a wide range of both feedforward and feedback movements. Here, we showed that SF muscle synergies are modulated on a much finer timescale (10 ms) than prior studies (Torres-Oviedo et al. 2006; Torres-Oviedo and Ting 2010) and that the same SF muscle synergies are recruited throughout the entire time course of muscle activity that extends beyond the end of the perturbation. In contrast, prior studies only investigated SF muscle synergies in a few coarse (75 ms) time bins during the initial postural response and did not include deceleration epochs that have more variable spatial and temporal patterns of muscle activation (Carpenter et al. 2005). We studied the entire time course of postural stabilization and found that despite the differences in body configuration and dynamics in later epochs, SF muscle synergies nonetheless had consistent structure across perturbation epochs but could be recruited differently from trial to trial, consistent with previous studies (Torres-Oviedo and Ting 2007). Similarly, SF muscle synergies have been shown to be modulated throughout voluntary tasks that alter limb configuration, including upper limb reaching movements (Cheung et al. 2009; Muceli et al. 2010). SF muscle synergies are also shared across motor tasks with different dynamics (Cheung et al. 2005; d'Avella and Bizzi 2005; Kargo et al. 2010). Moreover, SF muscle synergies are preserved after the removal of sensory feedback, but the temporal recruitment of muscle synergies is altered (Cheung et al. 2005). Similarly, in poststroke hemiparesis, the timing of SF muscle synergy recruitment during gait is impaired, but the structure of SF muscle synergies is similar to that found in healthy subjects (Clark et al. 2010).

Our results suggest that the temporal recruitment of SF muscle synergies during human balance control is constrained by low-dimensional task variables. Previously, constraints have been identified in the temporal structure of muscle activity using TF muscle synergies (Cappellini et al. 2006; Ivanenko et al. 2004, 2005); alternatively, no constraints on temporal structure have been applied when using SF muscle synergies (Hart and Giszter 2004; Saltiel et al. 2001; Torres-Oviedo and Ting 2007). Here we demonstrate that the temporal constraints on the recruitment of SF muscle synergies are decoupled from the spatial constraints in human postural control, as also shown in corrective movements in frog (Kargo and Giszter 2000) and deletions during fictive locomotion in decerebrate cats (McCrea and Rybak 2008). Recently, delayed feedback of CoM was shown to reconstruct the temporal activity of several individual muscles in unidirectional postural responses (Lockhart and Ting 2007; Welch and Ting 2008, 2009). We extend this work to show that SF muscle synergy recruitment is also modulated by task-level feedback both throughout and across trials, providing a hierarchical, low-dimensional organization of temporal features of muscle coordination. Our formulation is particularly useful in postural control, where the temporal recruitment patterns of muscle synergies are modifiable from trial to trial.

### *SF Versus TF Muscle Synergies*

We found that SF muscle synergies produced better data reconstructions when using a small number of components and yielded more physiologically interpretable results than TF muscle synergies. Because SF muscle synergies have different preferred directions of activation, only a subset of SF muscle synergies was necessary to reconstruct muscle activity for any given perturbation direction. Similarly, directional tuning is seen in many populations of cells in the nervous system (Georgopoulos et al. 1982; Hubel and Wiesel 1962; Weinstein et al. 1991). By contrast, a majority of TF muscle synergies were necessary to reconstruct muscle activity for any given

perturbation direction, regardless of the number of muscle synergies extracted (Fig. 5*B*). Increasing the number of TF muscle synergies resulted in components that were more finely localized in time yet were still recruited across all perturbation directions and muscles, ultimately achieving the resolution of the EMG signal. Because the same temporal commands are recruited across perturbation directions, the muscles recruited by TF components must be rearranged to account for the trial-by-trial variations in muscle recruitment both across and within perturbation directions (Fig. 6*B*). As a result, in a postural task, TF muscle synergies can only reveal muscle patterns at an instant in time. Thus it is difficult to interpret the

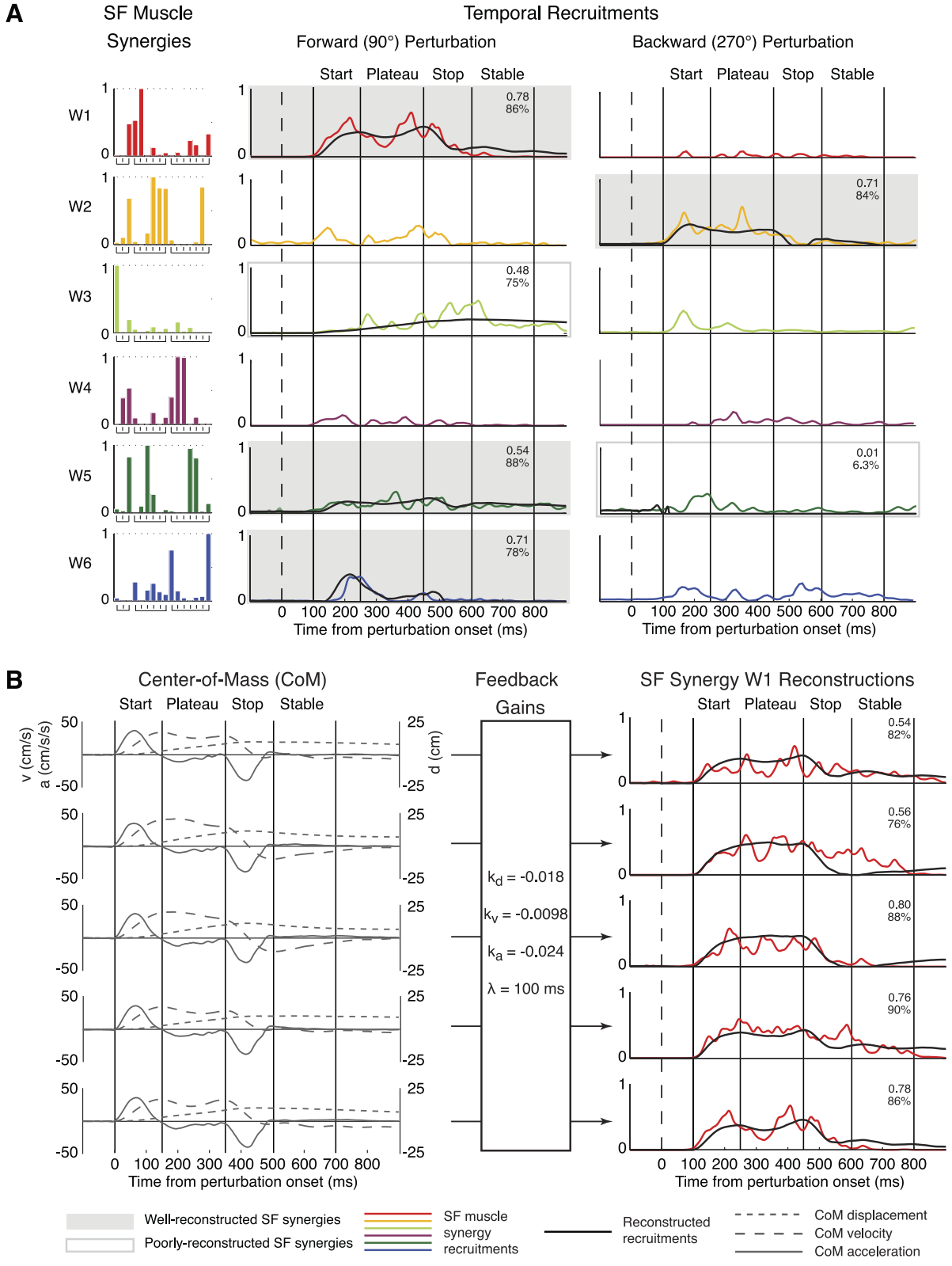

functional significance of temporal components in balance control. In contrast, SF muscle synergies can account for muscle activation patterns across trials and direction by relatively modest changes in their temporal recruitment patterns (Fig. 6*A*). Because SF muscle synergies can be variably recruited across trials and directions, SF muscle synergies reveal muscle coactivation patterns across a variety of timescales.

TF muscle synergies have been identified previously during feedforward tasks in which there may not have been sufficient dissociation of spatial and temporal features to identify the underlying structure of motor outputs. For example, the stereotyped cyclical motor patterns in locomotion make it difficult to dissociate spatial and temporal control of movement in walking tasks. Although aspects of locomotion are under feedback control (Kuo 2002; Lam et al. 2006; Reisman et al. 2005), the basic pattern of muscle activity is produced in a feedforward manner (Winter and Yack 1987). As such, muscle groups are activated at consistent phases of gait across walking speeds and gait patterns (Nilsson et al. 1985). Thus the data can appear to have either a fixed temporal or a fixed spatial structure. For example, the variability in EMG during locomotor tasks can be equally explained with TF (Ivanenko et al. 2004; Krouchev et al. 2006; Monaco et al. 2010) or SF (Clark et al. 2010) muscle synergies. Moreover, muscle activity during other voluntary tasks such as primate grasping or frog kicking, swimming, and jumping can be explained with muscle synergies with covarying spatiotemporal structure (d'Avella and Bizzi 2005; Overduin et al. 2008). In contrast to walking, perturbations separate and resolve such covariations (Kargo and Giszter 2000; Kargo et al. 2010); postural responses allow for the dissociation of spatial and temporal features of muscle coordination, which have similar temporal structure but recruit different muscles (Nashner 1976) across perturbation directions (Henry et al. 1998; Macpherson 1988). Moreover, very different temporal patterns can be elicited by varying perturbation characteristics, which can still be explained by CoM feedback (Lockhart and Ting 2007).

### *Neural Substrates for Recruitment and Structure of Muscle Synergies*

The mapping of task variables to muscle activity via SF muscle synergies is consistent with divergence in hierarchical neural structures. To produce desired motor outputs, multiple joints must be coordinated (Zajac and Gordon 1989). By coordinating muscles across joints, SF muscle synergies produce biomechanical functions to achieve motor outputs. The multijoint coordination patterns seen in SF muscle synergies mirror CNS structure: corticomotoneuronal, reticulospinal, and spinal cord interneurons are known to have divergent projections to multiple motoneurons (Jankowska 1992; Turton et al. 1993). Moreover, interneurons have been shown to project in patterns that match the structure of SF muscle synergies (Hart and Giszter 2010). Depending on the task, muscle synergies have been hypothesized to be encoded at different levels of the CNS, including motor cortex for grasping (d'Avella et al. 2008; Overduin et al. 2008), brain stem for postural control (Torres-Oviedo et al. 2006; Torres-Oviedo and Ting 2007), and spinal cord for locomotion (Drew et al. 2008) and other voluntary and reactive tasks (Bizzi et al. 1991; Giszter et al. 1993; Hart and Giszter 2010; Saltiel et al. 2001). Because the same muscle synergies can be used across tasks, it is likely that they can be accessed with multiple neural control schemes in a hierarchical fashion, regardless of their location in the nervous system.

The representation of global task variables such as CoM requires multisensory integration to estimate and reflects convergence in hierarchical neural structures. To estimate CoM, it is necessary to know the configuration of all body segments and their associated masses. Thus CoM must be estimated by integrating proprioceptive information across body segments with vestibular and/or visual information (Peterka 2002). Many diverse postural paradigms have suggested that CoM governs muscle activity during standing balance in a feedback manner (Gollhofer et al. 1989; Kuo 1995; Peterka 2000, 2002; van der Kooij and de Vlugt 2007). As a global task-level variable, CoM is more tightly regulated in postural control than local variables such as joint angles (Allum and Carpenter 2005; Brown et al. 2001; Gollhofer et al. 1989; Krishnamoorthy et al. 2003; Scholz and Schoner 1999). Task-level feedback is implicated in electrophysiological studies as well: in primate motor cortex, pyramidal neurons are found to respond to task-level variables during voluntary reaching such as movement direction, velocity, and end point force (Georgopoulos et al. 1986, 1992). Limb length and orientation can be assembled from afferent signals in both the dorsal root ganglia (Weber et al. 2007) and the dorsal spinocerebellar tract (Bosco et al. 1996).

Task-level variables provide a low-dimensional neural control scheme that may be mapped to individual muscles via low-dimensional muscle synergies. It has been proposed that the nervous system could make use of sensory feedback to estimate the body's state and achieve a desired movement trajectory through low-dimensional control (Todorov 2004). By using task-level feedback to recruit SF muscle synergies, it may be possible for the nervous system to reliably control task-level variables. Using SF muscle synergies, low-dimensional control has been demonstrated to be sufficient to simulate effective locomotion (Neptune et al. 2009). Kargo and Giszter (2010) showed that simulations of frog wiping trajectories are more accurate when using feedback modulation of SF muscle synergies than without proprioceptive feedback.

Fig. 9. Feedback model reconstruction of SF muscle synergy recruitment patterns. Data are shown for *subject 2*. *A*: reconstruction of recruitment patterns in a forward and backward perturbation. SF muscle synergies (W1–W6) are differentially recruited throughout A-P perturbations. Active SF muscle synergies (shaded) were reconstructed with a delayed feedback model based on CoM motion. W1, W2, and W6 were well-reconstructed across trials (mean $r^2 \geq 0.5$ or mean VAF $\geq 75\%$ for all trials). W2 was poorly reconstructed over trials. W5 was well-reconstructed in forward perturbations but poorly reconstructed in backward perturbations. Both W1 and W6 have major contributions from mono- and biarticular muscles affecting the trunk (REAB, RFEM, GMED). Reconstructions are only shown for 1 trial for ease of interpretation. Colored lines, SF muscle synergy recruitment patterns; black lines, feedback model reconstructions. *B*: reconstruction of muscle synergy W1 for all forward trials. Intertrial differences in SF muscle synergy recruitment can be accounted for by differences in CoM kinematics. Using a single set of feedback gains, the feedback model can account for trial-by-trial variability in recruitment for SF muscle synergies. Numbers indicate $r^2$ (*top*) and VAF (*bottom*) values for reconstructions. Gray lines, CoM kinematics; colored lines, muscle synergy recruitment patterns; black lines, feedback model reconstructions.

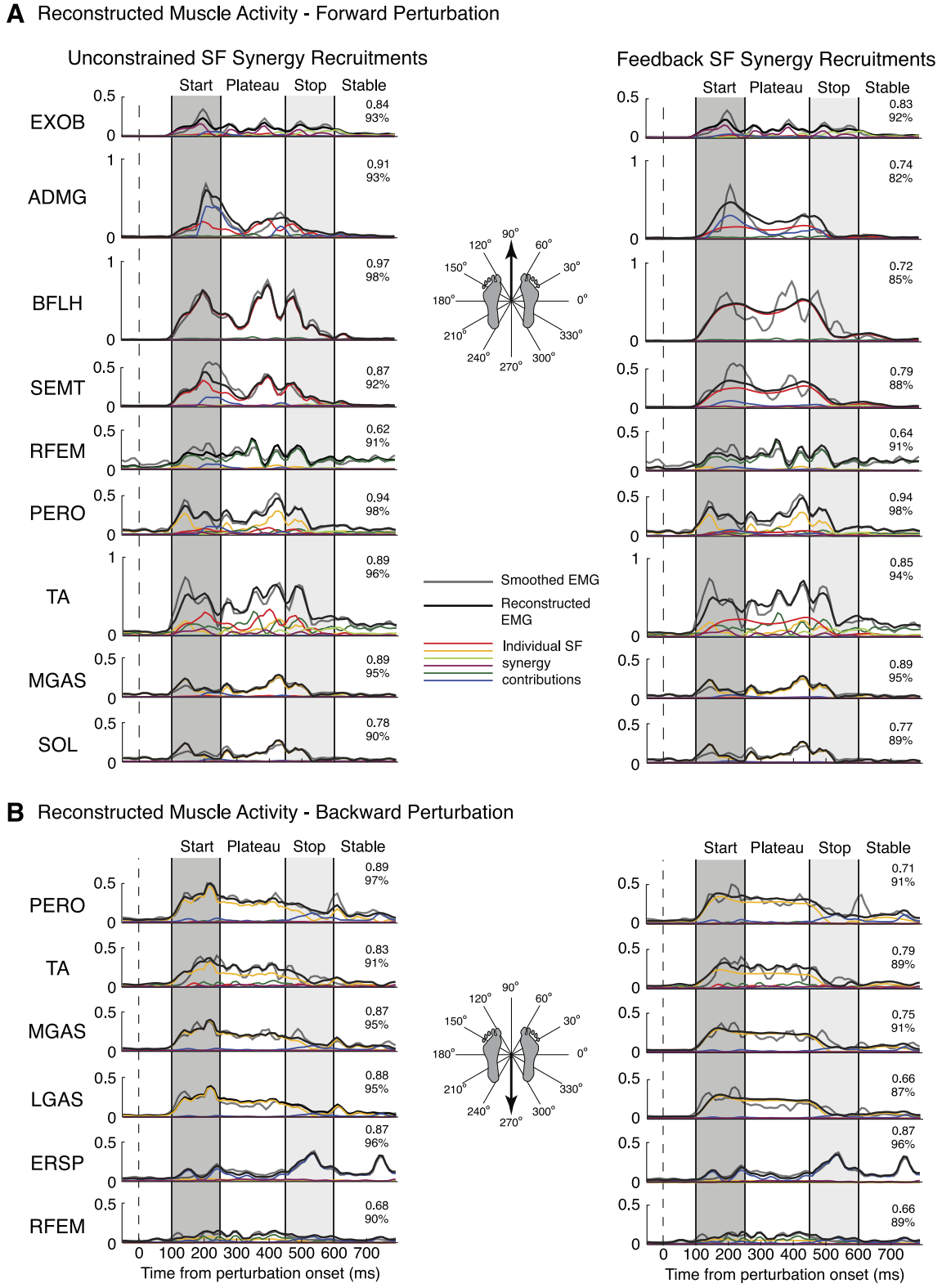


Fig. 10. Reconstruction of individual muscle activity with SF muscle synergy recruitment patterns determined from nonnegative matrix factorization (NNMF) (unconstrained, *left*) and the feedback model (*right*) for a forward (*A*) and a backward (*B*) perturbation. Data are shown for *subject 2*. Although recruitment patterns determined from NNMF explain the variability better than recruitment patterns determined from the feedback model, both methods of extraction have high correlation values for active muscles in A-P perturbations. Both SF muscle synergy recruitment patterns reconstructed muscle activation patterns significantly better than when using $N_{syn\text{-}T}$ ($P < 0.01$ for $r^2$ and VAF) or $N_{syn\text{-}S}$ ($P < 0.01$ for $r^2$) TF muscle synergy recruitment patterns (data not shown). Gray lines, smoothed EMG; black lines, reconstructed EMG; colored lines, individual SF muscle synergy contributions.

Berniker et al. (2009) also suggested that neural commands would be driven by task-level variables; simulations of SF muscle synergy recruitment using low-dimensional, task-level control provided a more accurate prediction of frog hindlimb muscle activity than other control schemes. In cat reaching, pyramidal tract neurons are found to discharge in a manner related to task dynamics and muscle synergy recruitment (Yakovenko et al. 2011).

### *Competing Influences on Muscle Activation During Standing Balance Control*

Aside from CoM, our results suggest that other task variables such as orientation may also be important for recruiting SF muscle synergies that had actions at the hip. Trunk orientation has been proposed as a competing task variable on postural responses (Kluzik et al. 2005; Macpherson et al. 1997; Massion 1994). Similarly, neurons in the reticular formation have been shown to respond to task-level variables such as orientation (Deliagina et al. 2008) or equilibrium (Schepens et al. 2008; Stapley and Drew 2009). Moreover, sensory feedback and descending control may have a greater influence on muscle activity at the hip because of the biomechanics of bipedal stance. However, muscle synergies with hip involvement were recruited in a manner inconsistent with changes in hip angle kinematics or vertical deviation. Thus local control of hip angle is unlikely to account for SF muscle synergy recruitment. As opposed to local variables, the nervous system may be integrating and responding to a combination of joint kinematics. Because joint torques are coupled across body segments during postural responses (Alexandrov et al. 1998), it is likely that the combinations of joint kinematics are integrated into a task-level variable, such as maintaining a vertical orientation of the lower limb or minimizing the overall bending of the joints.

In addition to recruiting SF muscle synergies, there may be other neural influences underlying muscle activation in human postural control. Despite the consistency of SF muscle synergies throughout perturbations, SF muscle synergy structure was slightly less consistent in later epochs versus earlier epochs. While SF muscle synergies may reflect an underlying neural structure for producing motor outputs, observed muscle activity is the result of a superposition of a variety of commands in the nervous system (Horak et al. 1997; Ting 2007). Later muscle activity could be due to descending cognitive influences that act at longer latencies, possibly via corticospinal loops and/or brain stem interactions (Jacobs and Horak 2007). Sensory feedback via local and/or global circuits may also affect muscle activity, since postural control is an ongoing task that is dependent on sensory cues for an estimate of body position and orientation (Macpherson et al. 1997; Massion 1994). Altered sensory feedback of multiple modalities has been known to modulate muscular patterns in postural responses (Honeycutt and Nichols 2010; Stapley et al. 2002, 2006), and sensory feedback has been shown to slightly alter the composition of SF muscle synergies (Cheung et al. 2005).

The deviations in our predictions from actual data may be explained in part by inherent methodological limitations of our analyses. Using NNMF, we performed SF muscle synergy analysis on 16 EMG signals during small epochs throughout the postural response. Because component analysis algorithms such as NNMF are used to parse out salient features of muscle coordination, more robust muscle synergies can be identified when the EMG variability is high. When the extraction epoch is reduced, the data set contains less EMG variability; as a result, SF muscle synergies identified from these smaller epochs can reflect smaller variations in EMG. Interestingly, additional SF muscle synergies were most often identified when extracted from early epochs that have most often been studied in postural responses (Henry et al. 1998; Macpherson 1988; Ting and Macpherson 2005; Torres-Oviedo and Ting 2007). Some of these previously identified SF muscle synergies may reflect smaller variations during these epochs and may be less indicative of the actual spatial structure of muscle coordination patterns. Additionally, the reconstructions of high-frequency oscillations in EMG activity and SF muscle synergy recruitment patterns were limited because we used low-frequency kinematic signals as inputs. Nevertheless, our reconstructions were still able to explain the majority of the variability in SF muscle synergy recruitment patterns, suggesting that higher-frequency variations in muscle synergy recruitment may not be significant. Finally, ramp-and-hold perturbations artificially correlate joint and CoM kinematics, making it difficult to establish truly independent correlations with SF muscle synergy activity. In a natural environment, these variables may be decoupled; alternative perturbations that decouple these variables (Kung et al. 2009) may need to be explored to better our understanding of neural control schemes.

## GRANTS

This work is supported by National Institutes of Health (NIH) Grant R01 NS-058322 to L. H. Ting. S. A. Safavynia is supported by a Medical Scientist Training Program Fellowship (NIH 5 T32 GM-08169-24).

## DISCLOSURES

No conflicts of interest, financial or otherwise, are declared by the author(s).

## AUTHOR CONTRIBUTIONS

Author contributions: S.A.S. and L.H.T. conception and design of research; S.A.S. performed experiments; S.A.S. analyzed data; S.A.S. and L.H.T. interpreted results of experiments; S.A.S. prepared figures; S.A.S. drafted manuscript; S.A.S. and L.H.T. edited and revised manuscript; S.A.S. and L.H.T. approved final version of manuscript.

## REFERENCES

**Alexandrov A, Frolov A, Massion J.** Axial synergies during human upper trunk bending. *Exp Brain Res* 118: 210–220, 1998.

**Allum JH, Carpenter MG.** A speedy solution for balance and gait analysis: angular velocity measured at the centre of body mass. *Curr Opin Neurol* 18: 15–21, 2005.

**Berniker M, Jarc A, Bizzi E, Tresch MC.** Simplified and effective motor control based on muscle synergies to exploit musculoskeletal dynamics. *Proc Natl Acad Sci USA* 106: 7601–7606, 2009.

**Bernstein N.** *The Coordination and Regulation of Movements*. New York: Pergamon, 1967.

**Bizzi E, Mussa-Ivaldi FA, Giszter SF.** Computations underlying the execution of movement: a biological perspective. *Science* 253: 287–291, 1991.

**Bosco G, Rankin AM, Poppele RE.** Representation of passive hindlimb postures in cat spinocerebellar activity. *J Neurophysiol* 76: 715–726, 1996.

**Brown LA, Jensen JL, Korff T, Woollacott MH.** The translating platform paradigm: perturbation displacement waveform alters the postural response. *Gait Posture* 14: 256–263, 2001.

**Cappellini G, Ivanenko YP, Poppele RE, Lacquaniti F.** Motor patterns in human walking and running. *J Neurophysiol* 95: 3426–3437, 2006.

**Carpenter MG, Thorstensson A, Cresswell AG.** Deceleration affects anticipatory and reactive components of triggered postural responses. *Exp Brain Res* 167: 433–445, 2005.

**Cheung VC, d'Avella A, Tresch MC, Bizzi E.** Central and sensory contributions to the activation and organization of muscle synergies during natural motor behaviors. *J Neurosci* 25: 6419–6434, 2005.

**Cheung VC, Piron L, Agostini M, Silvoni S, Turolla A, Bizzi E.** Stability of muscle synergies for voluntary actions after cortical stroke in humans. *Proc Natl Acad Sci USA* 106: 19563–19568, 2009.

**Chvatal SA, Torres-Oviedo G, Safavynia SA, Ting LH.** Common muscle synergies for control of center of mass and force in nonstepping and stepping postural behaviors. *J Neurophysiol* 106: 999–1015, 2011.

**Clark DJ, Ting LH, Zajac FE, Neptune RR, Kautz SA.** Merging of healthy motor modules predicts reduced locomotor performance and muscle coordination complexity post-stroke. *J Neurophysiol* 103: 844–857, 2010.

**d'Avella A, Bizzi E.** Shared and specific muscle synergies in natural motor behaviors. *Proc Natl Acad Sci USA* 102: 3076–3081, 2005.

**d'Avella A, Fernandez L, Portone A, Lacquaniti F.** Modulation of phasic and tonic muscle synergies with reaching direction and speed. *J Neurophysiol* 100: 1433–1454, 2008.

**Deliagina TG, Beloozerova IN, Zelenin PV, Orlovsky GN.** Spinal and supraspinal postural networks. *Brain Res Rev* 57: 212–221, 2008.

**Drew T, Kalaska J, Krouchev N.** Muscle synergies during locomotion in the cat: a model for motor cortex control. *J Physiol* 586: 1239–1245, 2008.

**Georgopoulos AP, Ashe J, Smyrnis N, Taira M.** The motor cortex and the coding of force. *Science* 256: 1692–1695, 1992.

**Georgopoulos AP, Kalaska JF, Caminiti R, Massey JT.** On the relations between the direction of two-dimensional arm movements and cell discharge in primate motor cortex. *J Neurosci* 2: 1527–1537, 1982.

**Georgopoulos AP, Schwartz AB, Kettner RE.** Neuronal population coding of movement direction. *Science* 233: 1416–1419, 1986.

**Giszter SF, Mussa-Ivaldi FA, Bizzi E.** Convergent force fields organized in the frog's spinal cord. *J Neurosci* 13: 467–491, 1993.

**Gollhofer A, Horstmann GA, Berger W, Dietz V.** Compensation of translational and rotational perturbations in human posture: stabilization of the centre of gravity. *Neurosci Lett* 105: 73–78, 1989.

**Hart CB, Giszter SF.** Modular premotor drives and unit bursts as primitives for frog motor behaviors. *J Neurosci* 24: 5269–5282, 2004.

**Hart CB, Giszter SF.** A neural basis for motor primitives in the spinal cord. *J Neurosci* 30: 1322–1336, 2010.

**Henry SM, Fung J, Horak FB.** EMG responses to maintain stance during multidirectional surface translations. *J Neurophysiol* 80: 1939–1950, 1998.

**Honeycutt CF, Nichols TR.** Disruption of cutaneous feedback alters magnitude but not direction of muscle responses to postural perturbations in the decerebrate cat. *Exp Brain Res* 203: 765–771, 2010.

**Horak FB, Henry SM, Shumway-Cook A.** Postural perturbations: new insights for treatment of balance disorders. *Phys Ther* 77: 517–533, 1997.

**Horak FB, Macpherson JM.** Postural orientation and equilibrium. In: *Handbook of Physiology. Exercise: Regulation and Integration of Multiple Systems* Bethesda, MD: Am Physiol Soc, 1996, sect. 12, p. 255–292.

**Hubel DH, Wiesel TN.** Receptive fields, binocular interaction and functional architecture in the cat's visual cortex. *J Physiol* 160: 106–154, 1962.

**Ivanenko YP, Cappellini G, Dominici N, Poppele RE, Lacquaniti F.** Coordination of locomotion with voluntary movements in humans. *J Neurosci* 25: 7238–7253, 2005.

**Ivanenko YP, Grasso R, Zago M, Molinari M, Scivoletto G, Castellano V, Macellari V, Lacquaniti F.** Temporal components of the motor patterns expressed by the human spinal cord reflect foot kinematics. *J Neurophysiol* 90: 3555–3565, 2003.

**Ivanenko YP, Poppele RE, Lacquaniti E.** Five basic muscle activation patterns account for muscle activity during human locomotion. *J Physiol* 556: 267–282, 2004.

**Jacobs JV, Horak FB.** Cortical control of postural responses. *J Neural Transm* 114: 1339–1348, 2007.

**Jankowska E.** Interneuronal relay in spinal pathways from proprioceptors. *Prog Neurobiol* 38: 335–378, 1992.

**Kargo WJ, Giszter SF.** Rapid correction of aimed movements by summation of force-field primitives. *J Neurosci* 20: 409–426, 2000.

**Kargo WJ, Ramakrishnan A, Hart CB, Rome LC, Giszter SF.** A simple experimentally based model using proprioceptive regulation of motor primitives captures adjusted trajectory formation in spinal frogs. *J Neurophysiol* 103: 573–590, 2010.

**Kluzik J, Horak FB, Peterka RJ.** Differences in preferred reference frames for postural orientation shown by after-effects of stance on an inclined surface. *Exp Brain Res* 162: 474–489, 2005.

**Krishnamoorthy V, Latash ML, Scholz JP, Zatsiorsky VM.** Muscle synergies during shifts of the center of pressure by standing persons. *Exp Brain Res* 152: 281–292, 2003.

**Krouchev N, Kalaska JF, Drew T.** Sequential activation of muscle synergies during locomotion in the intact cat as revealed by cluster analysis and direct decomposition. *J Neurophysiol* 96: 1991–2010, 2006.

**Kung UM, Horlings CG, Honegger F, Duysens JE, Allum JH.** Control of roll and pitch motion during multi-directional balance perturbations. *Exp Brain Res* 194: 631–645, 2009.

**Kuo AD.** An optimal control model for analyzing human postural balance. *IEEE Trans Biomed Eng* 42: 87–101, 1995.

**Kuo AD.** The relative roles of feedforward and feedback in the control of rhythmic movements. *Motor Control* 6: 129–145, 2002.

**Lam T, Anderschitz M, Dietz V.** Contribution of feedback and feedforward strategies to locomotor adaptations. *J Neurophysiol* 95: 766–773, 2006.

**Lee DD, Seung HS.** Learning the parts of objects by non-negative matrix factorization. *Nature* 401: 788–791, 1999.

**Lockhart DB, Ting LH.** Optimal sensorimotor transformations for balance. *Nat Neurosci* 10: 1329–1336, 2007.

**Macpherson JM.** Strategies that simplify the control of quadrupedal stance. II. Electromyographic activity. *J Neurophysiol* 60: 218–231, 1988.

**Macpherson JM, Fung J, Jacobs R.** Postural orientation, equilibrium, and the spinal cord. *Adv Neurol* 72: 227–232, 1997.

**Massion J.** Postural control system. *Curr Opin Neurobiol* 4: 877–887, 1994.

**McCrea DA, Rybak IA.** Organization of mammalian locomotor rhythm and pattern generation. *Brain Res Rev* 57: 134–146, 2008.

**McKay JL, Ting LH.** Functional muscle synergies constrain force production during postural tasks. *J Biomech* 41: 299–306, 2008.

**Monaco V, Ghionzoli A, Micera S.** Age-related modifications of muscle synergies and spinal cord activity during locomotion. *J Neurophysiol* 104: 2092–2102, 2010.

**Muceli S, Boye AT, d'Avella A, Farina D.** Identifying representative synergy matrices for describing muscular activation patterns during multidirectional reaching in the horizontal plane. *J Neurophysiol* 103: 1532–1542, 2010.

**Nashner LM.** Adapting reflexes controlling the human posture. *Exp Brain Res* 26: 59–72, 1976.

**Neptune RR, Clark DJ, Kautz SA.** Modular control of human walking: a simulation study. *J Biomech* 42: 1282–1287, 2009.

**Nilsson J, Thorstensson A, Halbertsma J.** Changes in leg movements and muscle activity with speed of locomotion and mode of progression in humans. *Acta Physiol Scand* 123: 457–475, 1985.

**Overduin SA, d'Avella A, Roh J, Bizzi E.** Modulation of muscle synergy recruitment in primate grasping. *J Neurosci* 28: 880–892, 2008.

**Peterka RJ.** Postural control model interpretation of stabilogram diffusion analysis. *Biol Cybern* 82: 335–343, 2000.

**Peterka RJ.** Sensorimotor integration in human postural control. *J Neurophysiol* 88: 1097–1118, 2002.

**Reisman DS, Block HJ, Bastian AJ.** Interlimb coordination during locomotion: what can be adapted and stored? *J Neurophysiol* 94: 2403–2415, 2005.

**Saltiel P, Wyler-Duda K, D'Avella A, Tresch MC, Bizzi E.** Muscle synergies encoded within the spinal cord: evidence from focal intraspinal NMDA iontophoresis in the frog. *J Neurophysiol* 85: 605–619, 2001.

**Schepens B, Stapley P, Drew T.** Neurons in the pontomedullary reticular formation signal posture and movement both as an integrated behavior and independently. *J Neurophysiol* 100: 2235–2253, 2008.

**Scholz JP, Schoner G.** The uncontrolled manifold concept: identifying control variables for a functional task. *Exp Brain Res* 126: 289–306, 1999.

**Stapley PJ, Drew T.** The pontomedullary reticular formation contributes to the compensatory postural responses observed following removal of the support surface in the standing cat. *J Neurophysiol* 101: 1334–1350, 2009.

**Stapley PJ, Ting LH, Hulliger M, Macpherson JM.** Automatic postural responses are delayed by pyridoxine-induced somatosensory loss. *J Neurosci* 22: 5803–5807, 2002.

**Stapley PJ, Ting LH, Kuifu C, Everaert DG, Macpherson JM.** Bilateral vestibular loss leads to active destabilization of balance during voluntary head turns in the standing cat. *J Neurophysiol* 95: 3783–3797, 2006.

**Ting LH.** Dimensional reduction in sensorimotor systems: a framework for understanding muscle coordination of posture. *Prog Brain Res* 165: 299–321, 2007.

**Ting LH, Chvatal SA.** Decomposing muscle activity in motor tasks: methods and interpretation. In: *Motor Control: Theories, Experiments, and Applications*, edited by Danion F, Latash ML. Oxford: Oxford Univ. Press, 2010, p. 102–138.

**Ting LH, Macpherson JM.** A limited set of muscle synergies for force control during a postural task. *J Neurophysiol* 93: 609–613, 2005.

**Todorov E.** Optimality principles in sensorimotor control. *Nat Neurosci* 7: 907–915, 2004.

**Torres-Oviedo G, Macpherson JM, Ting LH.** Muscle synergy organization is robust across a variety of postural perturbations. *J Neurophysiol* 96: 1530–1546, 2006.

**Torres-Oviedo G, Ting LH.** Muscle synergies characterizing human postural responses. *J Neurophysiol* 98: 2144–2156, 2007.

**Torres-Oviedo G, Ting LH.** Subject-specific muscle synergies in human balance control are consistent across different biomechanical contexts. *J Neurophysiol* 103: 3084–3098, 2010.

**Tresch MC, Cheung VC, d'Avella A.** Matrix factorization algorithms for the identification of muscle synergies: evaluation on simulated and experimental data sets. *J Neurophysiol* 95: 2199–2212, 2006.

**Tresch MC, Saltiel P, Bizzi E.** The construction of movement by the spinal cord. *Nat Neurosci* 2: 162–167, 1999.

**Turton A, Fraser C, Flament D, Werner W, Bennett KMB, Lemon RN.** Organization of cortico-motoneuronal projections from the primary motor cortex: evidence for task-related function in monkey and man. In: *Spasticity—Mechanisms and Management*, edited by Thilmann A, Burke DJ, Rymer WZ. Berlin: Springer, 1993, p. 8–24.

**van der Kooij H, de Vlugt E.** Postural responses evoked by platform pertubations are dominated by continuous feedback. *J Neurophysiol* 98: 730–743, 2007.

**Weber DJ, Stein RB, Everaert DG, Prochazka A.** Limb-state feedback from ensembles of simultaneously recorded dorsal root ganglion neurons. *J Neural Eng* 4: S168–S180, 2007.

**Weinstein JM, Balaban CD, VerHoeve JN.** Directional tuning of the human presaccadic spike potential. *Brain Res* 543: 243–250, 1991.

**Welch TD, Ting LH.** A feedback model explains the differential scaling of human postural responses to perturbation acceleration and velocity. *J Neurophysiol* 101: 3294–3309, 2009.

**Welch TD, Ting LH.** A feedback model reproduces muscle activity during human postural responses to support-surface translations. *J Neurophysiol* 99: 1032–1038, 2008.

**Winter DA.** *Biomechanics and Motor Control of Human Movement*. Hoboken, NJ: Wiley, 2005.

**Winter DA, Yack HJ.** EMG profiles during normal human walking: stride-to-stride and inter-subject variability. *Electroencephalogr Clin Neurophysiol* 67: 402–411, 1987.

**Yakovenko S, Krouchev NI, Drew T.** Sequential activation of motor cortical neurons contributes to intralimb coordination during reaching in the cat by modulating muscle synergies. *J Neurophysiol* 105: 388–409, 2011.

**Zajac FE, Gordon ME.** Determining muscle's force and action in multi-articular movement. *Exerc Sport Sci Rev* 17: 187–230, 1989.

**Zar JH.** *Biostatistical Analysis*. Upper Saddle River, NJ: Prentice-Hall, 1999, p. 663.